A Novel Type of Organometallic 2-R-2,4-dihydro-1*H*- 3,1-benzoxazines with R = $[M(\eta^5\text{-}C_5H_4)(CO)_3]$ (M = Re or Mn) units. Experimental and Computational Studies of the Effect of the Substituent R on the Ring-Chain Tautomerism.

Juan Oyarzo,[a] Ramón Bosque,[b] Patricia Toro,[a] Carlos P. Silva,[c] Rodrigo Arancibia,[d] Mercè Font-Bardía,[e] Vania Artigas,[a] Carme Calvis,[f] Ramon Messeguer,[f] A. Hugo Klahn,[a,*] Concepción López [b,*]

[a] *Instituto de Química, Pontificia Universidad Católica de Valparaíso, Casilla 4059, Valparaíso, Chile.*

[b] *Secció de Química Inorgànica del Departament de Química Inorgànica i Orgànica, Facultat de Química, Universitat de Barcelona, Martí I Franquès 1-11. E-08028-Barcelona, Spain.*

[c] *Departamento de Química de los Materiales, Facultad de Química y Biología, Universidad de Santiago de Chile, Soft Matter Research-Technology Center, SMAT-C, Av. B. O*'Higgins 3363, Casilla 40, Correo 33, Santiago, Chile.

[d] *Laboratorio de Química Inorgánica y Organometálica, Departamento de Química Analítica e Inorgánica, Facultad de Ciencias Químicas, Universidad de Concepción, Concepción, Chile.*

[e] *Unitat de Difracció de Raig-X, Centres Científics i Tecnològics (CCiT), Universitat de Barcelona, Solé i Sabaris, 1-3, E-08028-Barcelona, Spain.*

[f] *Biomed Division, Health & Biomedicine Unit, LEITAT Technological Center, Parc Científic de Barcelona, Edifici Hèlix, Baldiri i Reixach 13-21, E-08028-Barcelona, Spain.*

Supporting Information

(47 pages)

Supporting information contents:

1.- Supplementary Figures

Figure S1. A) High resolution mass spectrum (HRMS) and **B)** electron impact mass spectrum of the solid isolated in the reaction between [Re(η^5-C_5H_4-CHO)$(CO)_3$] and the 2-aminobenzylalcohol. This product was identified by X-ray crystal diffraction as **6c** (see text).

Figure S2. IR spectrum of compound **6c**.

Figure S3. ^{1}H-NMR spectrum (in $CDCl_3$) of the raw material isolated in the reaction between equimolar amounts of [Mn(η^5-C_5H_4-CHO)$(CO)_3$] and the 2-aminobenzylalcohol in refluxing benzene for 12 h, showing the coexistence of several products. The expansion of the low field region shows the signals due to the protons of the aldehyde and the imine forms. The broad resonance in the range $3.5<\delta<4.0$ indicates the presence of the amine; while the typical pattern of the resonances due to the O–CH_2 protons of the closed form, that appear as a doublet of doublets are also detected between 4.6 and 5.1 ppm (see inset on the right hand side).

Figure S4. A) High resolution mass spectrum (HRMS) and **B)** electron impact mass spectrum of compound **6d** (see text).

Figure S5. IR spectrum of compound **6d**.

Figure S6. Atom numbering scheme for NMR studies.

Figure S7. ^{1}H-NMR spectrum of compound **6c** (in acetonitrile-d_3 at 298 K). Expansion of selected regions of the spectrum are also presented in order to include the assignments of the resonances of the closed form (**6c**) and to show the coexistence of the imine form as a minor component. Signals marked with an asterisk are due to the imine form (**5c**).

Figure S8. ^{1}H-NMR spectrum of compound **6d** (in acetonitrile-d_3 at 298 K). Expansions of selected regions of the spectrum are included in order to include the assignments of the resonances of the closed form (**6d**) and to show the coexistence of the imine form as a minor component. Signals marked with purple asterisk are due to the imine form (**5d**).

Figure S9. ^{13}C{^{1}H}- NMR spectrum of compound **6c** in acetonitrile-d_3 at 298 K.

Figure S10. ^{13}C{^{1}H}- NMR spectrum of compound **6d** in acetonitrile-d_3 at 298 K.

Figure S11. [^{1}H-^{1}H]-NOESY spectrum of compound **6c** in acetonitrile-d_3 at 298 K.

Figure S12. [^{1}H-^{1}H]-NOESY spectrum of compound **6d** in acetonitrile-d_3 at 298 K.

Figure S13. [^{1}H-^{13}C]-HSQC spectrum of compound **6c** in acetonitrile-d_3 at 298 K.

Figure S14. [^{1}H-^{13}C]-HSQC spectrum of compound **6d** in acetonitrile-d_3 at 298 K.

Figure S15. [^{1}H-^{13}C]-HMBC spectrum of compound **6c** in acetonitrile-d_3 at 298 K.

Figure S16. [^{1}H-^{13}C]-HMBC spectrum of compound **6d** in acetonitrile-d_3 at 298 K.

Figure S17. ^{1}H-NMR spectrum of compound **6c** (in CD_2Cl_2 at 298 K) and an expansion of the spectrum showing the signal due to the imine proton of the open form (**5c**).

Figure S18. ^{1}H-NMR spectrum of compound **6d** (in CD_2Cl_2 at 298 K). Expansions of selected regions of the spectrum are included in order to show the signal due to the imine proton of the open form **5d** and to ease the identification of the resonances and their assignment. Signals marked with an asterisk are due to the imine form **5d.**

Figure S19. (A) ^{1}H-NMR spectra of a freshly prepared solution of compound **6a** in CD_2Cl_2 and after different periods of storage (t = 4 h, t = 24 h at 298 K). (**B**) ^{1}H-NMR spectrum of the same sample after 30 h of storage at 298 K and an expansion showing the presence of **5a**, **6a** and ferrocenecarboxaldehyde.

Figure S20. (**A**) ^{1}H-NMR spectrum of a freshly prepared solution of compound **6b** in CD_2Cl_2 at 298 and after different periods of storage (t = 4 h, 24 h at 298 K). (**B**) ^{1}H-NMR spectrum of the same sample after 30 h of storage at 298 K and an expansion showing the presence of **5b**, **6b** and benzaldehyde.

Figure S21. ^{1}H-NMR spectrum of compound **6c** in benzene-d_6 at 298 K.

Figure S22. ^{1}H-NMR spectrum of compound **6d** benzene-d_6 at 298 K.

Figure S23. ^{13}C{^{1}H} -NMR spectra of compound **6c** in (**A**) CD_2Cl_2 or (**B**) in benzene-d_6 at 298 K.

Figure S24. ^{13}C{^{1}H} -NMR spectra of compound **6d** in (**A**) CD_2Cl_2 or (**B**) in benzene-d_6 at 298 K.

Figure S25. ^{1}H-NMR spectrum of a freshly prepared solution of compound **6c** in DMSO-d_6 at 298 and after different periods of storage (*t*). For *t* = 10 months the spectra showed additional resonances (marked with a yellow arrow) that indicate the presence of a minor component.

Figure S26. ^{1}H-NMR spectrum of a freshly prepared solution of compound **6d** in DMSO-d_6 at 298 and after different periods of storage (*t*).

Figure S27. ^{1}H-NMR and ^{13}C{^{1}H} (bottom) NMR spectra (300 MHz) of the aldimine [Re{(η^5-C_5H_4)-CH=N-(C_6H_4-2-OH)}$(CO)_3$] (**7c**) in $CDCl_3$ at 298 K.

Figure S28. ^{1}H-NMR spectra (300 MHz) of the aldimine [Mn{(η^5-C_5H_4)-CH=N-(C_6H_4-2-OH)}$(CO)_3$] (**7d**) in $CDCl_3$ at 298 K.

Figure S29. ^{1}H-NMR spectra (300 MHz) of a freshly prepared solution of aldimine [Re{(η^5-C_5H_4)-CH=N-(C_6H_4-2-OH)}$(CO)_3$] (**7c**) in DMSO-d_6 at 298 K (top) and after different periods of storage (*t*) {*t* = 4 h (middle) and 24 h (bottom)}.

Figure S30. ^{1}H-NMR spectra (300 MHz) of a freshly prepared solution of aldimine [Mn{(η^5-C_5H_4)-CH=N-(C_6H_4-2-OH)}$(CO)_3$] (**7d**) in DMSO-d_6 at 298 K (top) and after different periods of storage (*t*) {*t* = 4 h (middle) and 24 h (bottom)}.

Figure S31. UV-vis. spectra of compounds **6a-6d** in CH_2Cl_2 at 298 K.

2.- Supplementary Tables

Table S1. Crystal data and details of the refinement of the crystal structures of the 2-ferrocenyl, 2,4-dihydro-1*H*-3,1-benzoxazine (**6a**) and its 2-cyrhetrenyl- or 2-cymantrenyl-analogues (**6c** and **6d,** respectively).

Table S2. Final atomic coordinates for the optimized geometry of imine R-CH=N-(C_6H_4-2-CH_2OH), [with R = (η^5-C_5H_5)Fe(η^5-C_5H_4), (**5a**)].

Table S3. Final atomic coordinates for the optimized geometry of imine R-CH=N-(C_6H_4-2-CH_2OH)] [with R = Ph, (**5b**)].

Table S4. Final atomic coordinates for the optimized geometry of the R-CH=N-(C_6H_4-2-CH_2OH) with R = Re(η^5- C_5H_4)$(CO)_3$, (**5c**).

Table S5. Final atomic coordinates for the optimized geometry of the R-CH=N-(C_6H_4-2-CH_2OH) with R = Mn(η^5- C_5H_4)$(CO)_3$, (**5d**).

Table S6. Final atomic coordinates for the optimized geometry of the 2-ferrocenyl 2,4-dihydro-1*H*-3,1-benzoxazine (**6a**).

Table S7. Final atomic coordinates for the optimized geometry of 2-phenyl 2,4-dihydro-1*H*-3,1 benzoxazine (**6b**).

Table S8. Final atomic coordinates for the optimized geometry of the 2-cyrhetrenyl 2,4-dihydro-1*H*-3,1-benzoxazine compound (**6c**).

Table S9. Final atomic coordinates for the optimized geometry of the open form 2-cymanentryl 2,4-dihydro-1*H*-3,1-benzoxazine (**6d**).

Table S10. Calculated distances between the imine nitrogen and atoms of the pendant –OH moiety in the imines R-CH=N-(C_6H_4-2-CH_2OH) **5a-5d**, the Mulliken charges on the atoms involved in the 6-*endo* trig process and differences between their Mulliken charges.

Table S11. **A)** Calculated electronic energies (*E* in hartrees) for the imine forms R-CH=N-(C_6H_4-2-CH_2OH) (**5a-5d**) and their corresponding: 2-R-2,4-dihydro-1*H*-3,1-benzoxazines (**6a-6d**) in vacuum and in CH_2Cl_2, and free energy (*G*) calculated for both tautomers at 25 °C under identical experimental conditions; **B)** Differences between the electronic energies (ΔE) and free energies (ΔG) (in kcal/mol) of the imine forms R-CH=N-(C_6H_4-2-CH_2OH) (**5a-5d**) and those obtained for their corresponding tautomers 2-R-2,4-dihydro-1*H*-3,1 Benzoxazines (**6a-6d**), with the same R group, under identical conditions in vacuum and in CH_2Cl_2 and the calculated values of the free energy of the reactions $\boldsymbol{6}_i \rightarrow \boldsymbol{5}_i$.

Table S12. Calculated energy (in eV) of the HOMO and LUMO orbitals [$E_{(HOMO)}$ and $E_{(LUMO)}$, respectively] and the energy gap [$E_{gap} = E_{(LUMO)} - E_{(HOMO)}$ (in eV)] for the closed forms **6a-6d**, shown below and Mulliken charges on selected atoms.

Table S13. Absorption spectroscopic data for 2-R-2,4-dihydro-1*H*-3,1-benzoxazines (**6a-6d**) in CH_2Cl_2 at 298 K. Wavelengths (λ_i, in nm) and logarithms of the extinction coefficients (log ε_i (ε_i in M^{-1} cm^{-1})).[a]

1.-SUPPLEMENTARY FIGURES

Figure S1. A) High resolution mass spectrum (HRMS) and **B)** electron impact mass spectrum of the solid isolated in the reaction between [Re(η^5-C_5H_4-CHO)$(CO)_3$] and the 2-aminobenzylalcohol. This product was identified by X-ray crystal diffraction as **6c** (see text).

A

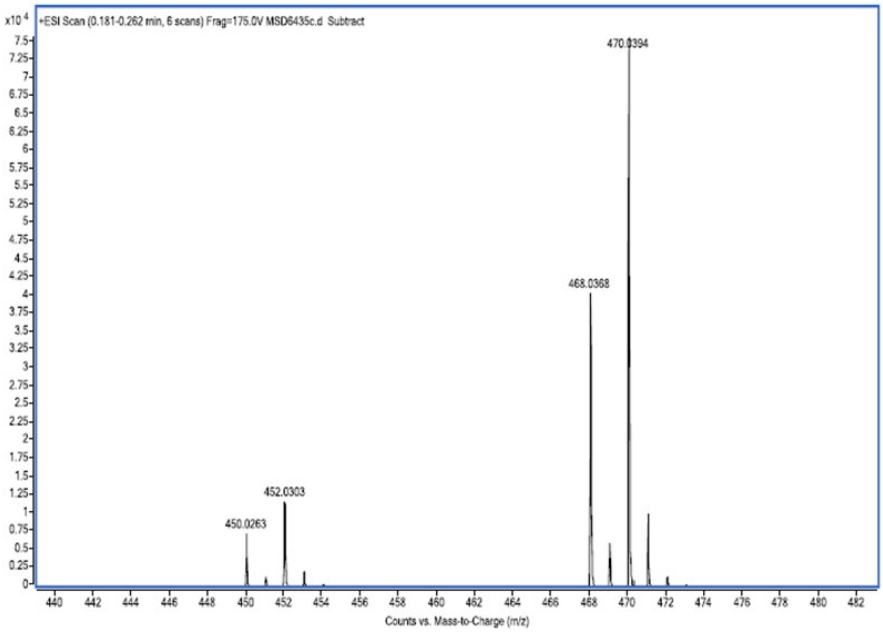

B

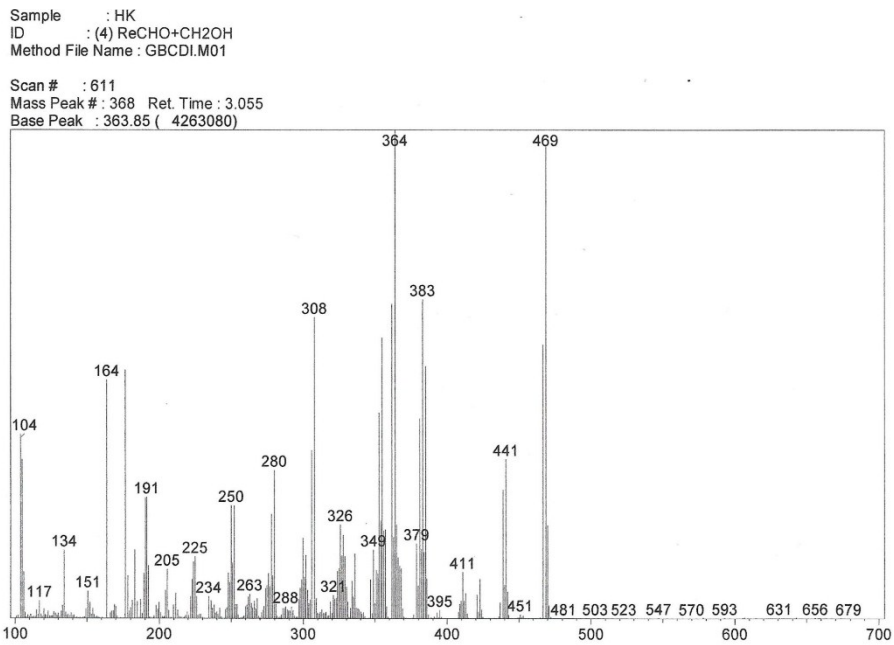

Figure S2. IR spectrum of compound **6c**.

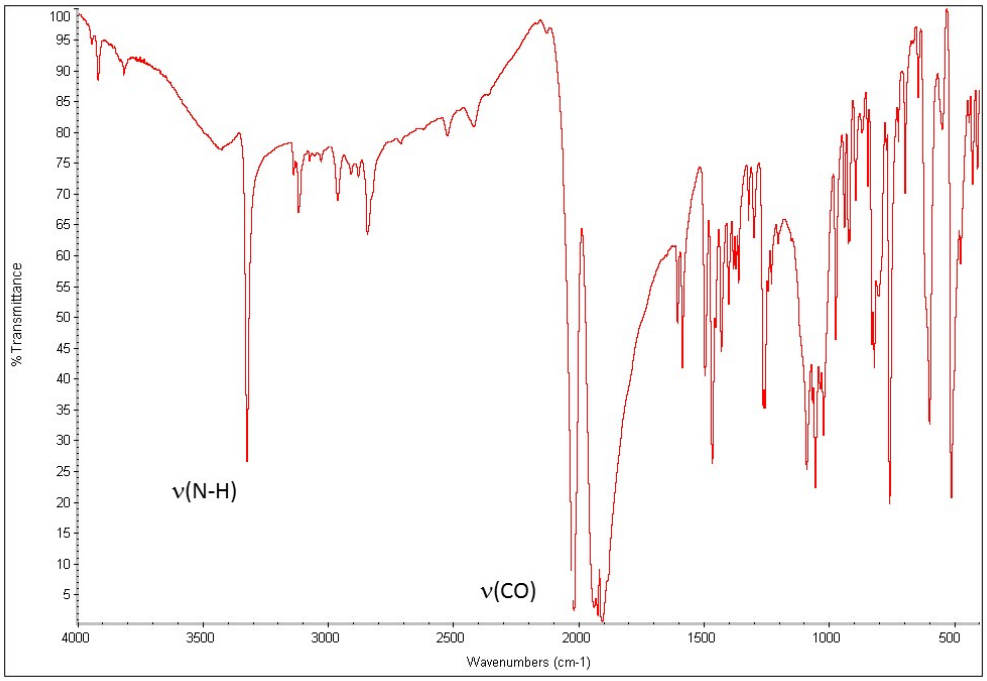

Figure S3. ^{1}H-NMR spectrum (in $CDCl_3$) of the raw material isolated in the reaction between equimolar amounts of [Mn(η^5-C_5H_4-CHO)$(CO)_3$] and the 2-aminobenzylalcohol in refluxing benzene for 12 h, showing the coexistence of several products. The expansion of the low field region shows the signals due to the protons of the aldehyde and the imine forms. The broad resonance in the range 3.5<δ<4.0 ppm indicates the presence of the amine; while the typical pattern of the resonances due to H^7 protons of the -OCH_2-unit of the closed form, (that appear as a doublet of doublets) are also detected between 4.6 and 5.1 ppm (see inset on the right hand side).

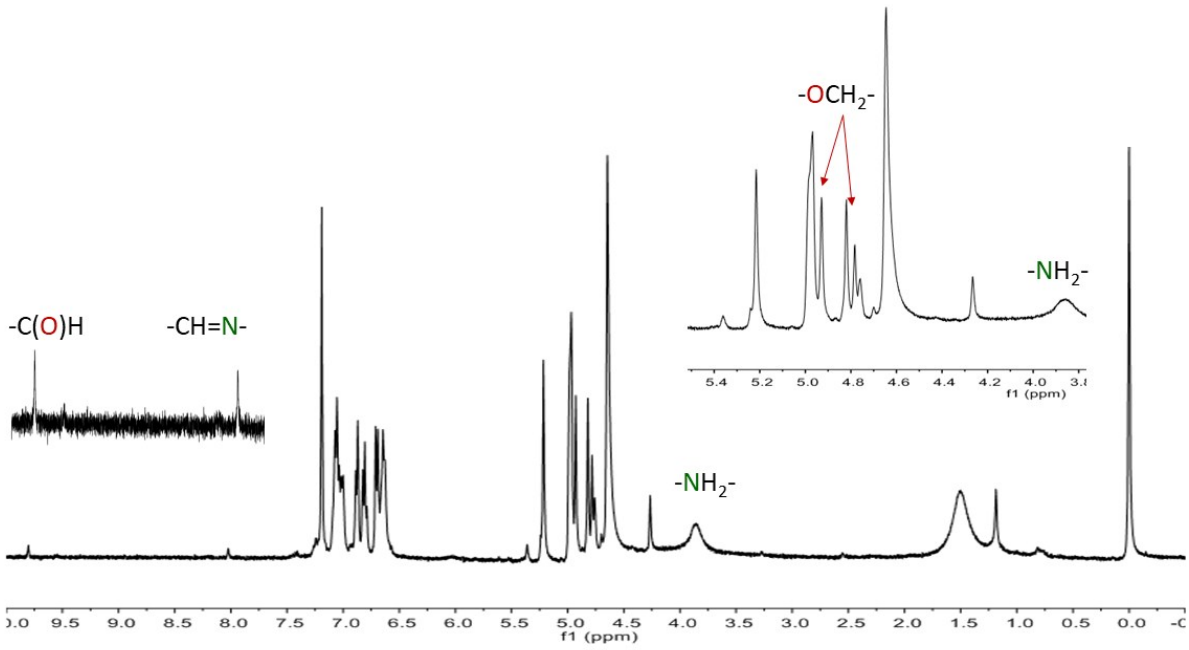

Figure S4. **A)** High resolution mass spectrum (HRMS) and **B)** electron impact mass spectrum of compound **6d.**

A

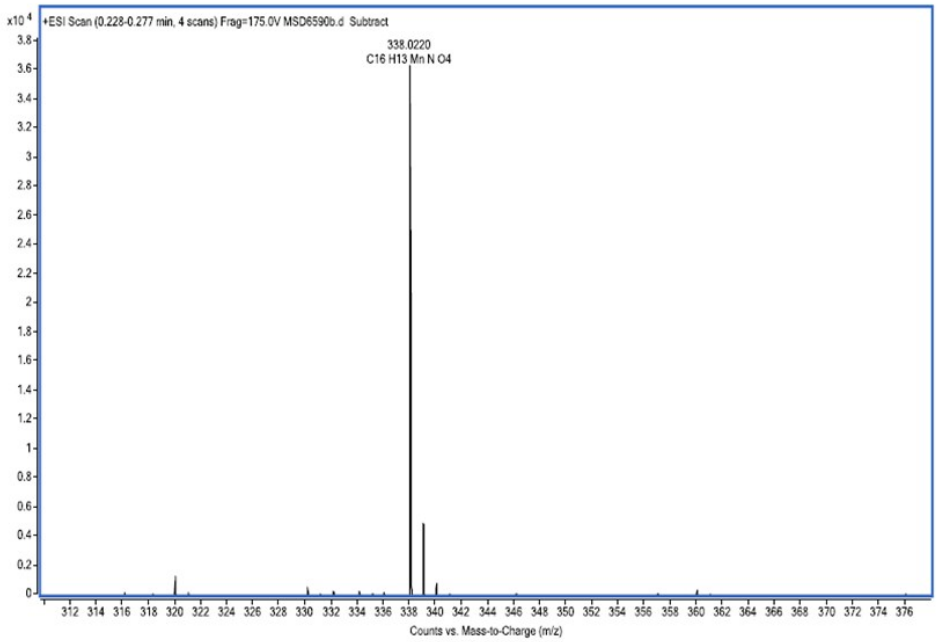

B

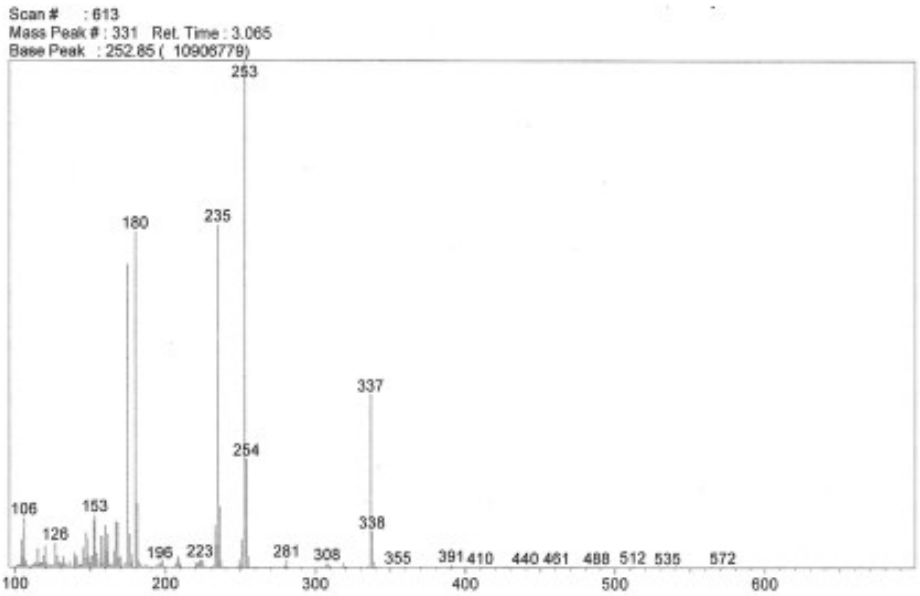

Figure S5. IR spectrum of compound **6d**.

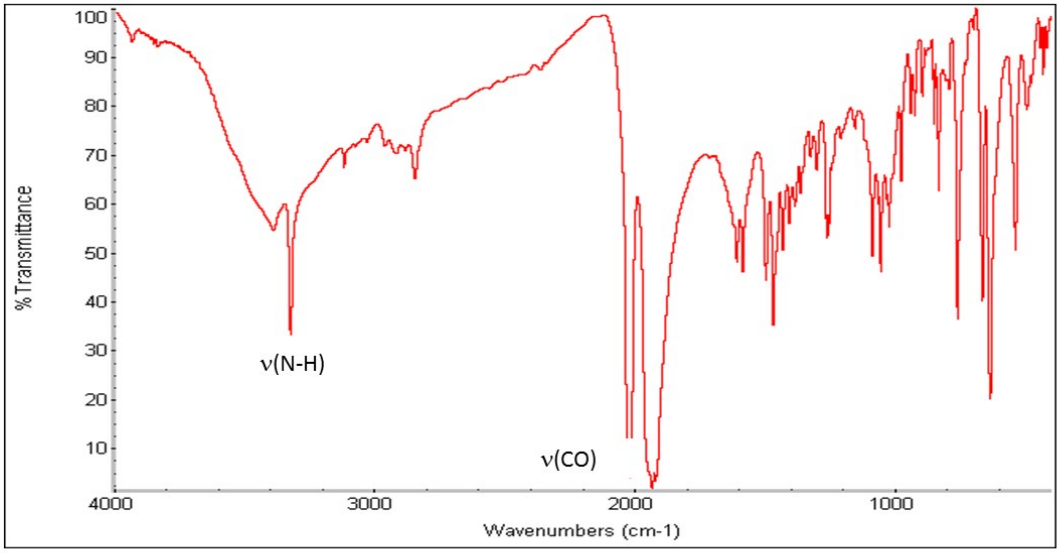

Figure S6. Atom numbering scheme for NMR studies (Green arrows indicate NOE peaks detected in the [^{1}H-^{1}H] NOESY spectra of compounds **6c** and **6d** in acetonitrile–d_3 solution at 298 K).

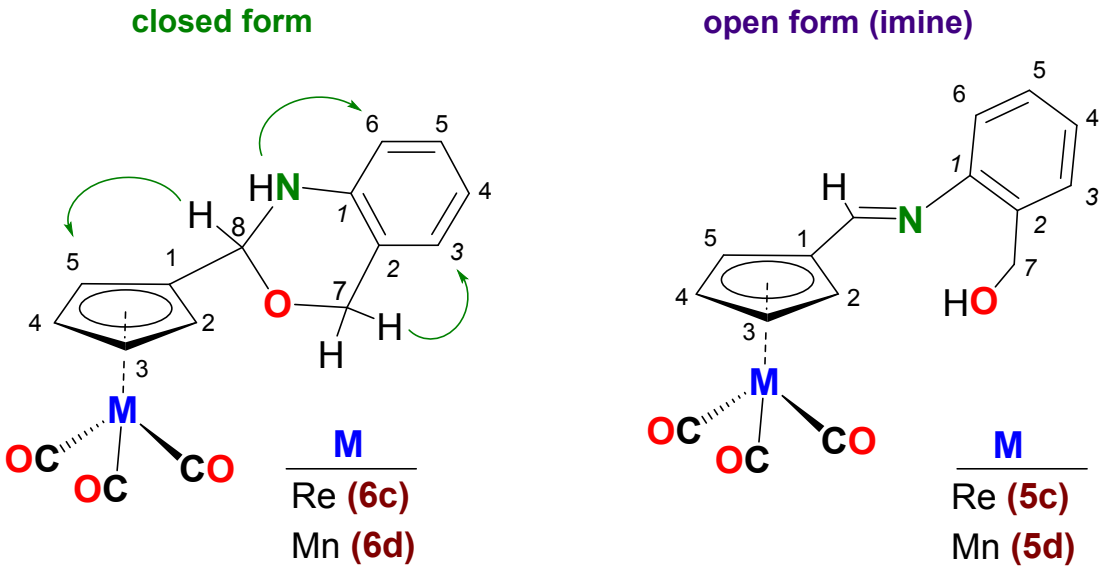

Figure S7. ^{1}H-NMR spectrum of compound **6c** (in acetonitrile-d_3 at 298 K). Expansion of selected regions of the spectrum are also presented in order to include the assignments of the resonances of the closed form (**6c**) and to show the coexistence of the imine form as a minor component. Signals marked with an asterisk are due to the imine form (**5c**).

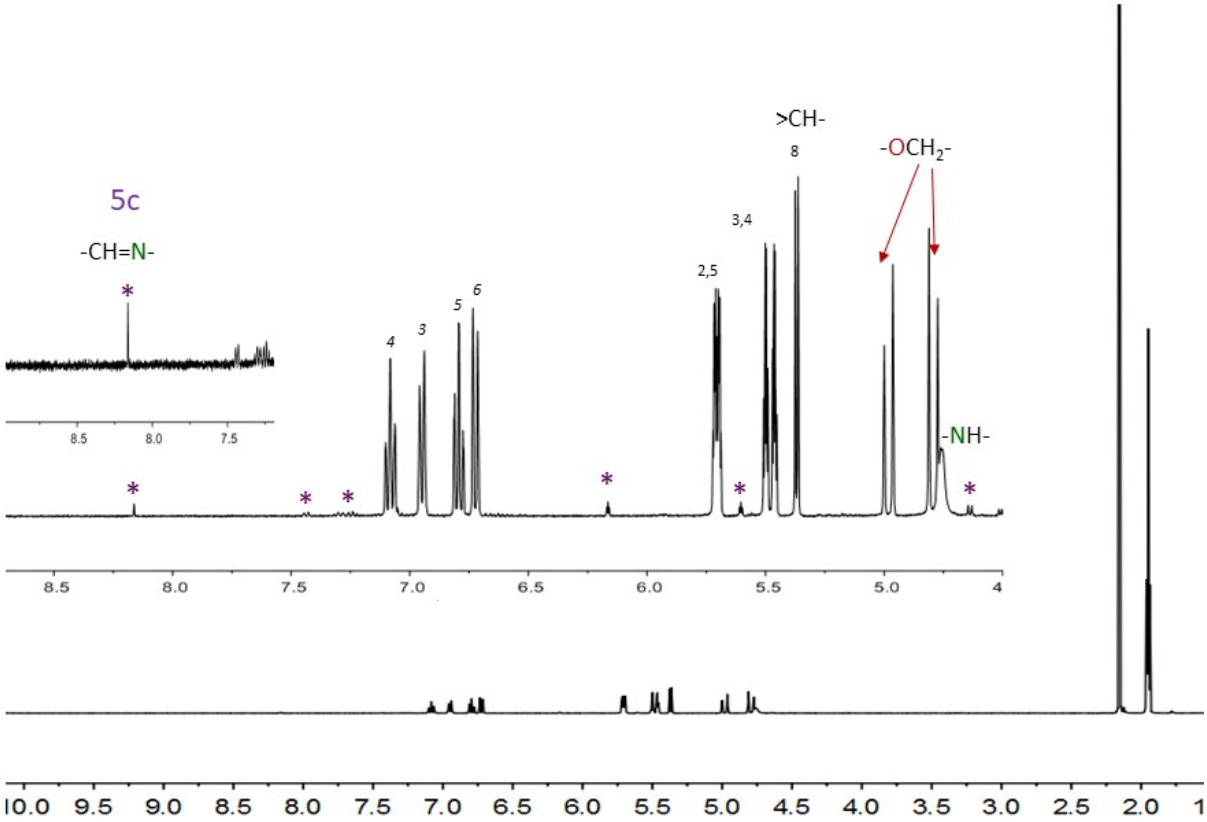

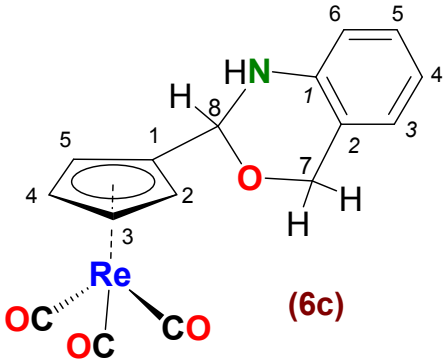

(6c)

Figure S8. ^{1}H-NMR spectrum of compound **6d** (in acetonitrile-d_3 at 298 K). Expansions of selected regions of the spectrum are included in order to include the assignments of the resonances of the closed form (**6d**) and to show the coexistence of the imine form as a minor component. Signals marked with purple asterisk are due to the imine form (**5d**).

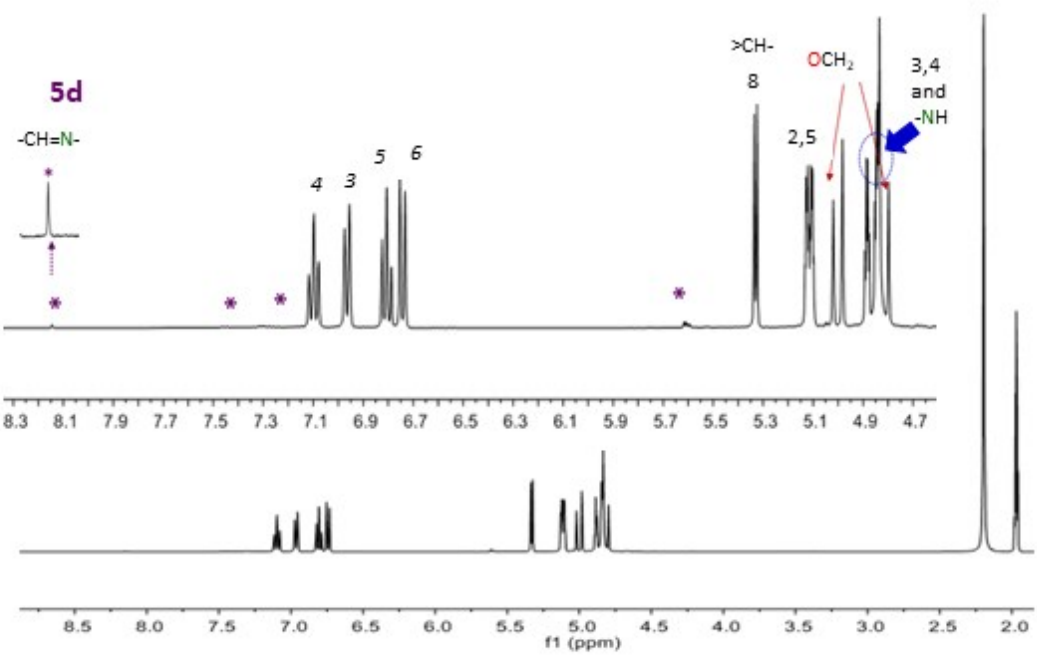

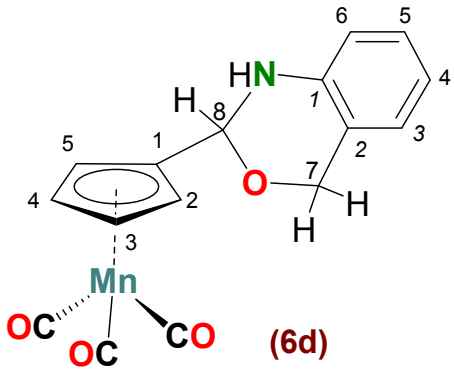

Figure S9. $^{13}C\{^{1}H\}$-NMR spectrum of compound **6c** (in acetonitrile-d_3 at 298 K). Expansions of selected regions of the spectrum are shown to include the assignments of the resonances of the closed form (**6c**).

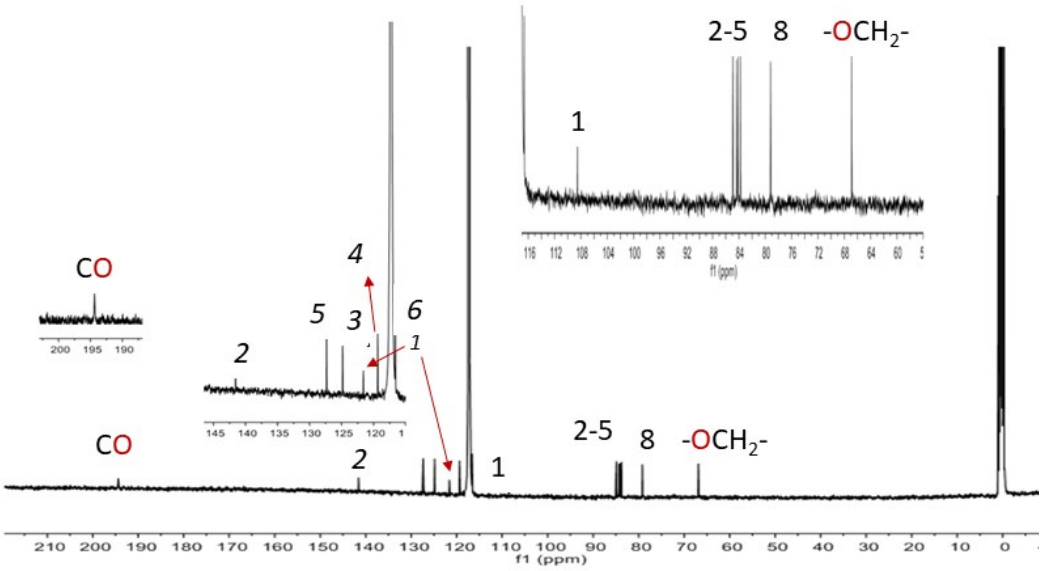

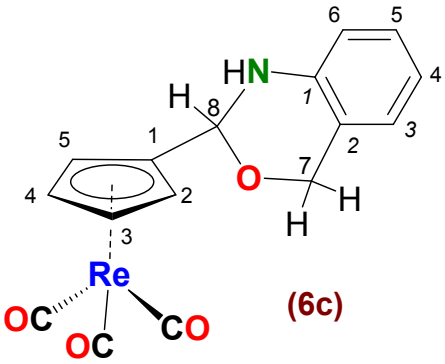

Figure S10. $^{13}C\{^{1}H\}$-NMR spectrum of compound **6d** (in acetonitrile-d_3 at 298 K). Expansions of selected regions of the spectrum are shown in order to include the assignments of the resonances of the closed form (**6d**).

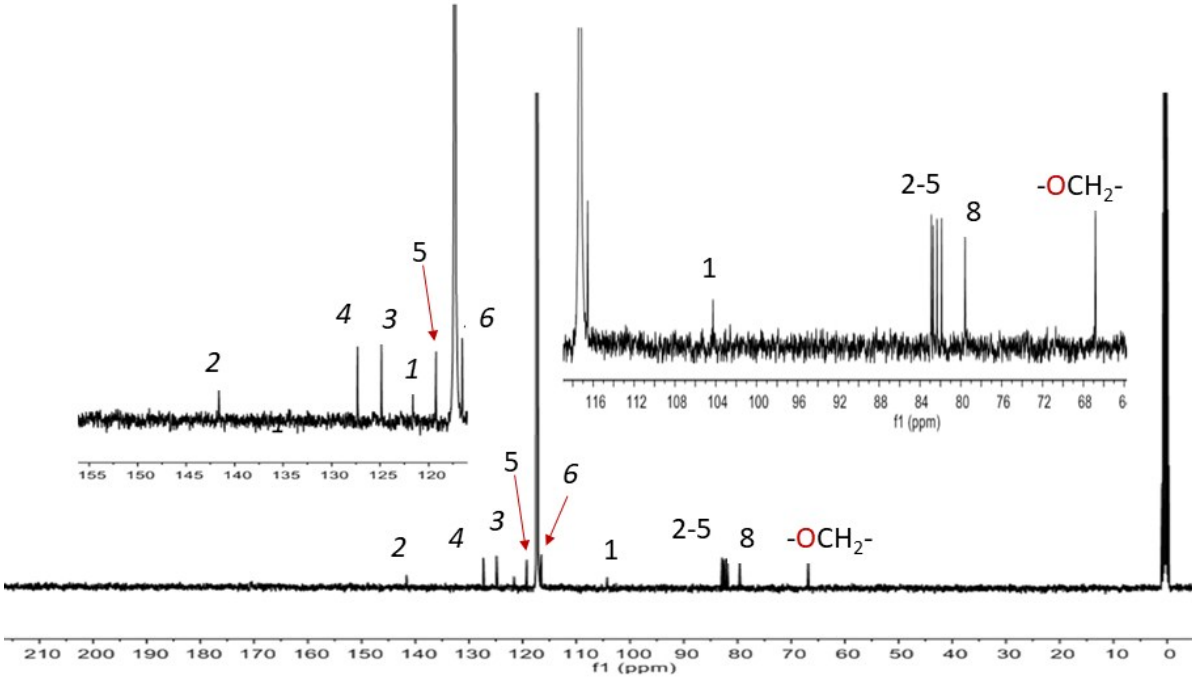

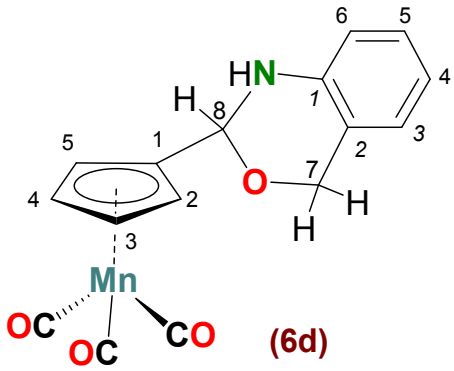

Figure S11. [^{1}H-^{1}H]-NOESY spectrum of compound **6c** in acetonitrile-d_3 at 298 K.

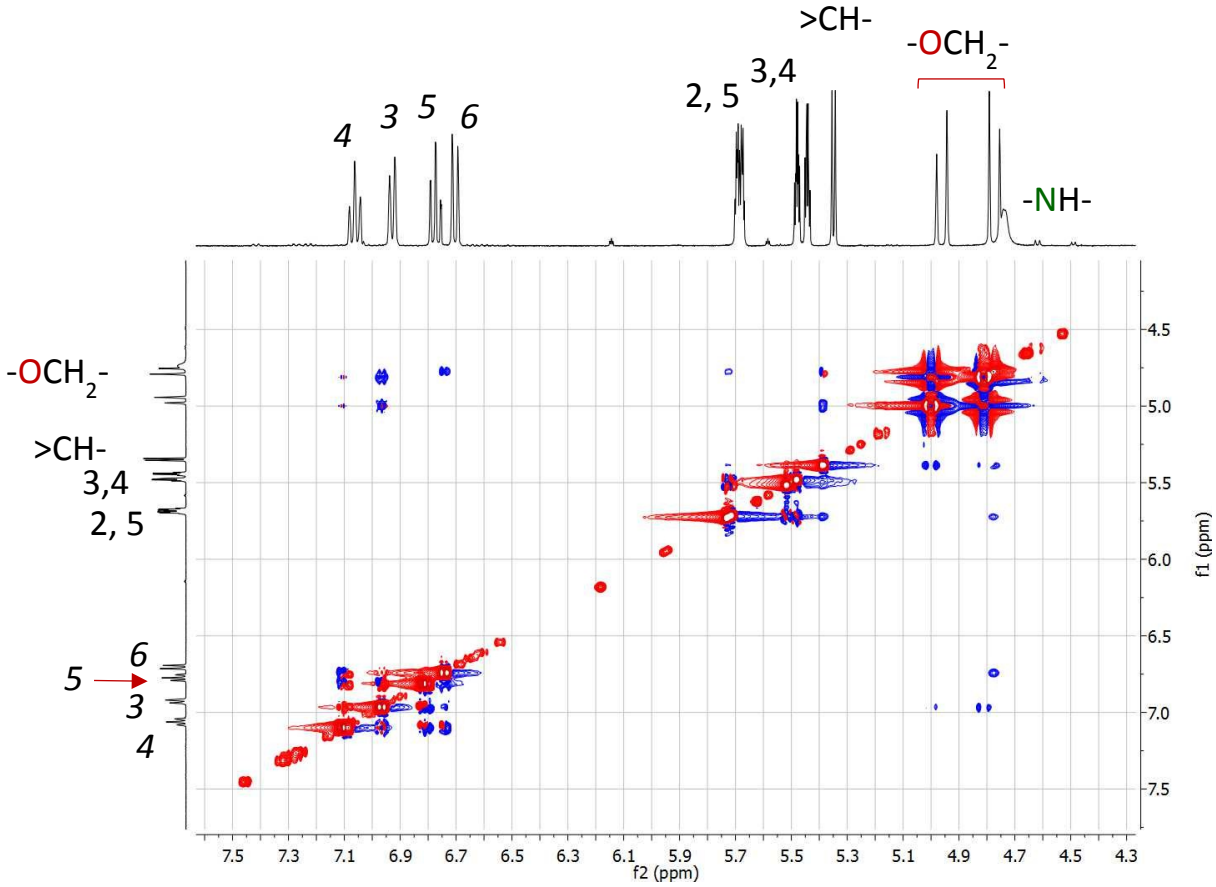

Figure S12. [^{1}H-^{1}H]-NOESY spectrum of compound **6d** in acetonitrile-d_3 at 298 K.

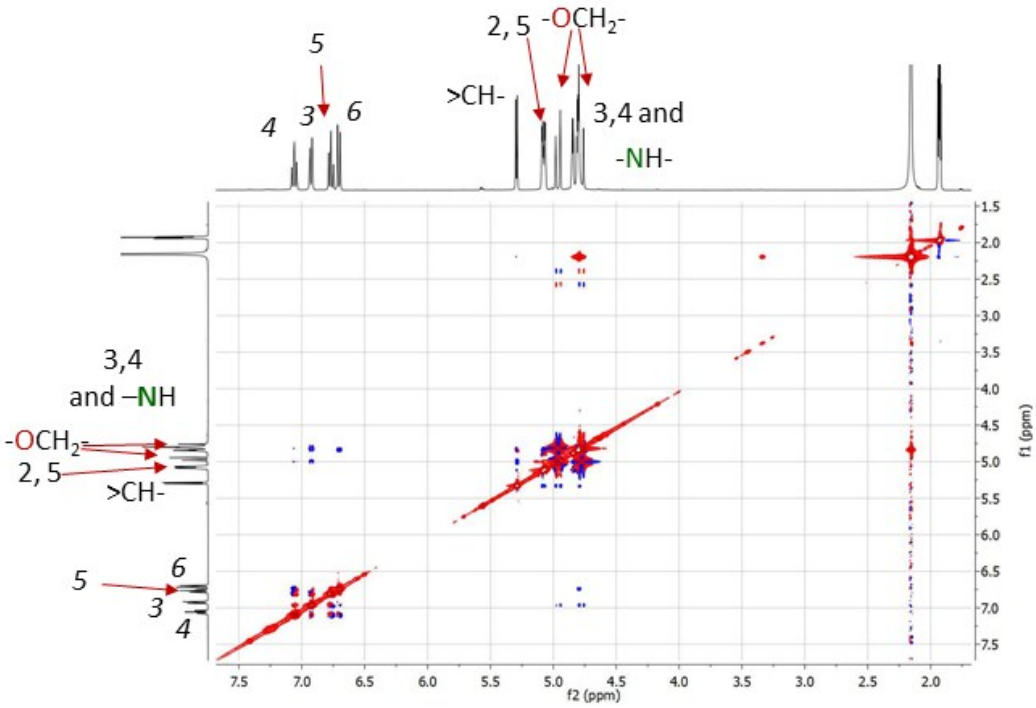

Figure S13. [^{1}H-^{13}C]-HSQC spectrum of compound **6c** in acetonitrile-d_3 at 298 K.

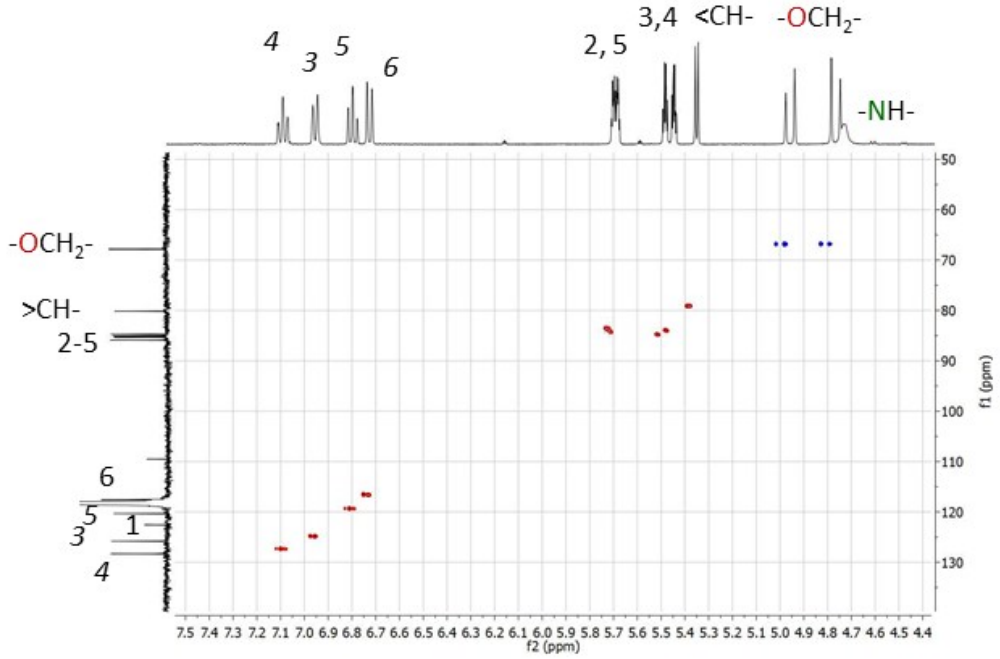

Figure S14. [^{1}H-^{13}C]-HSQC spectrum of compound **6d** in acetonitrile-d_3 at 298 K

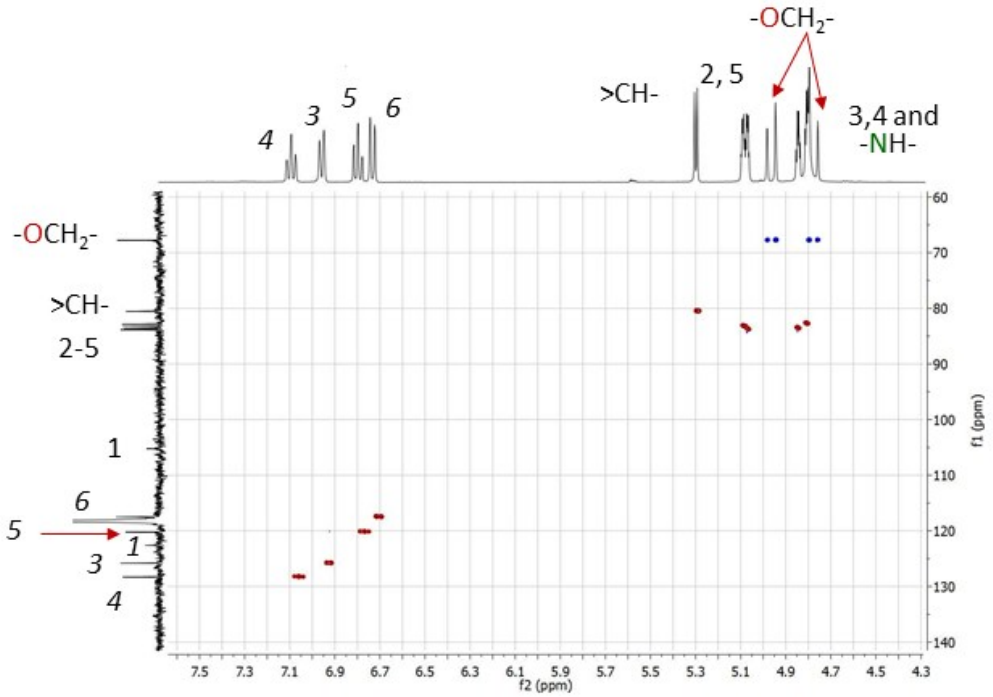

Figure S15. [^{1}H-^{13}C]-HMBC spectrum of compound **6c** in acetonitrile-d_3 at 298 K

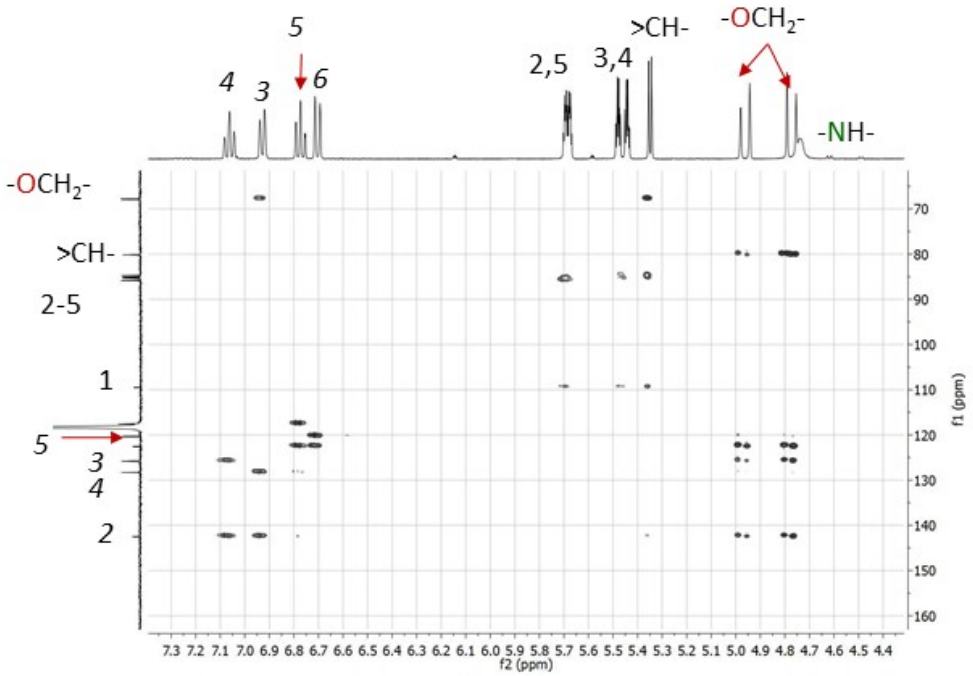

Figure S16. [^{1}H-^{13}C]-HMBC spectrum of compound **6c** in acetonitrile-d_3 at 298 K

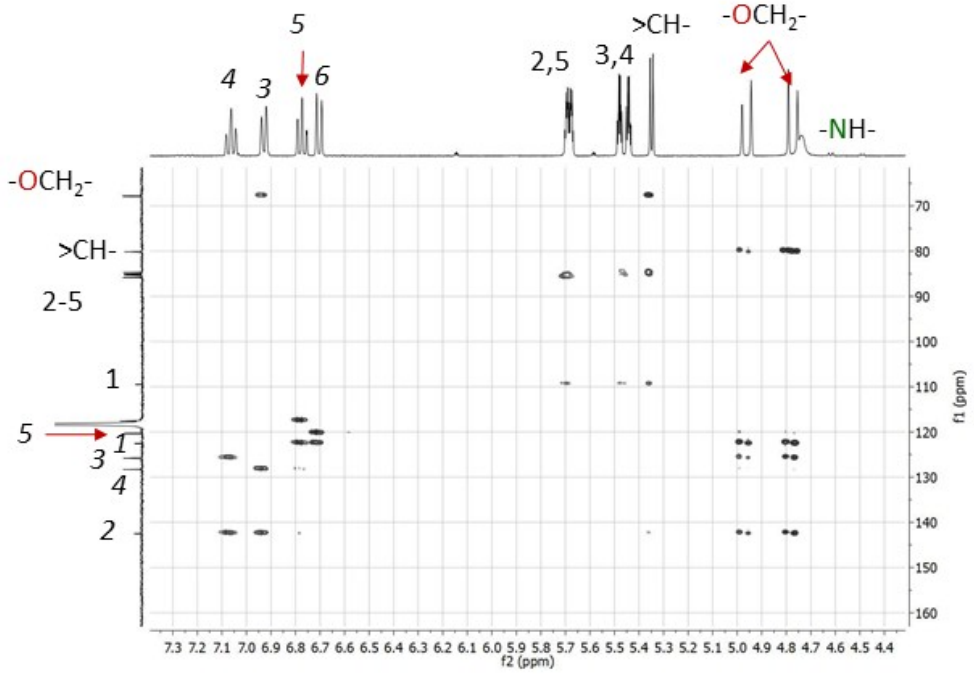

Figure S17. ^{1}H-NMR spectrum of compound **6c** (in CD_2Cl_2 at 298 K) and an expansion of the spectrum showing the signal due to the imine proton of the open form (**5c**).

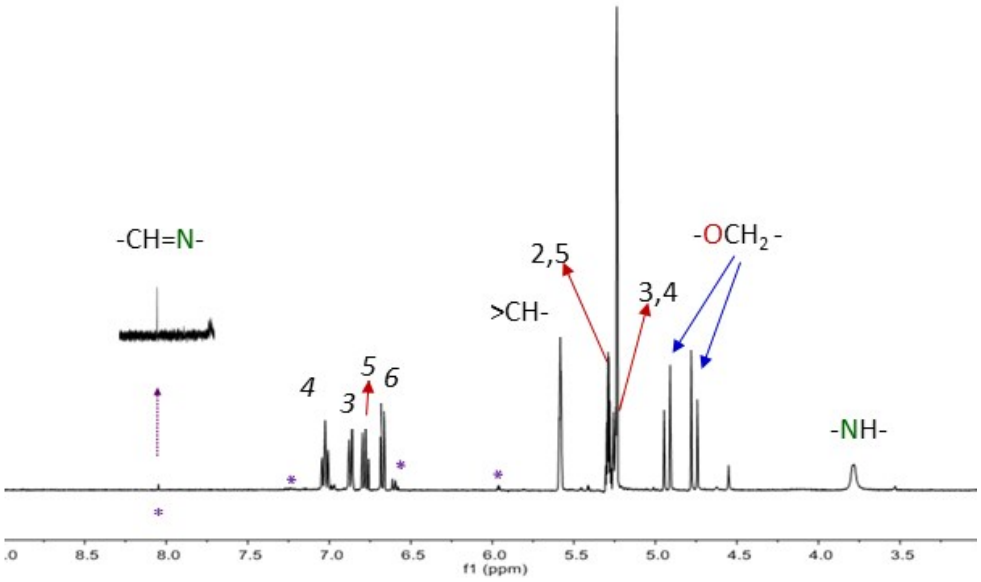

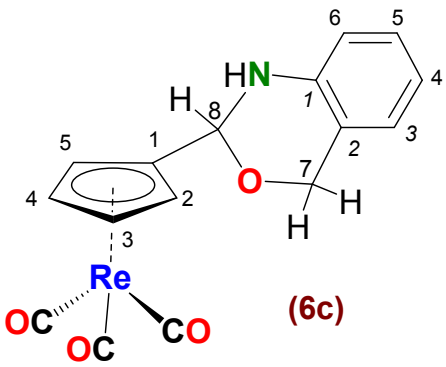

(6c)

Figure S18. ^{1}H-NMR spectrum of compound **6d** (in CD_2Cl_2 at 298 K). Expansions of selected regions of the spectrum are included in order to show the signal due to the imine proton of the open form **5d** and to ease the identification of the resonances and their assignment. Signals marked with an asterisk are due to the imine form **5d**

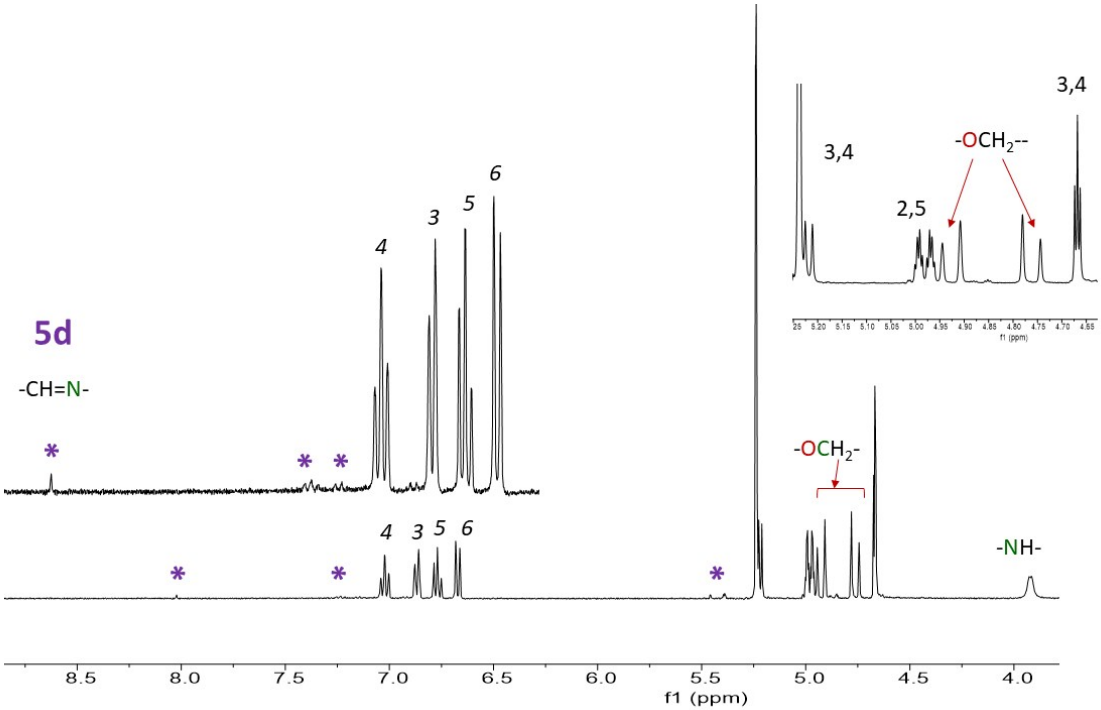

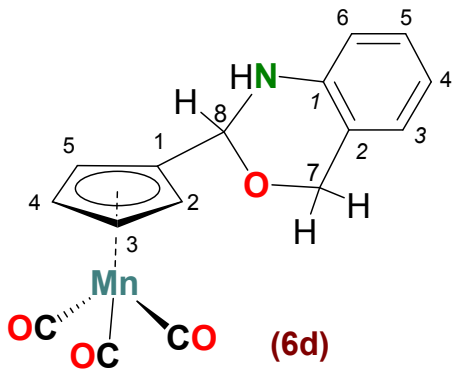

Figure S19. **(A)** ^{1}H-NMR spectra of a freshly prepared solution of compound **6a** in CD_2Cl_2 and after different periods of storage (t = 4 h, t = 24 h at 298 K). (**B**) ^{1}H-NMR spectrum of the same sample after 30 h of storage at 298 K and an expansion showing the presence of **5a**, **6a** and ferrocenecarboxaldehyde.

(A)

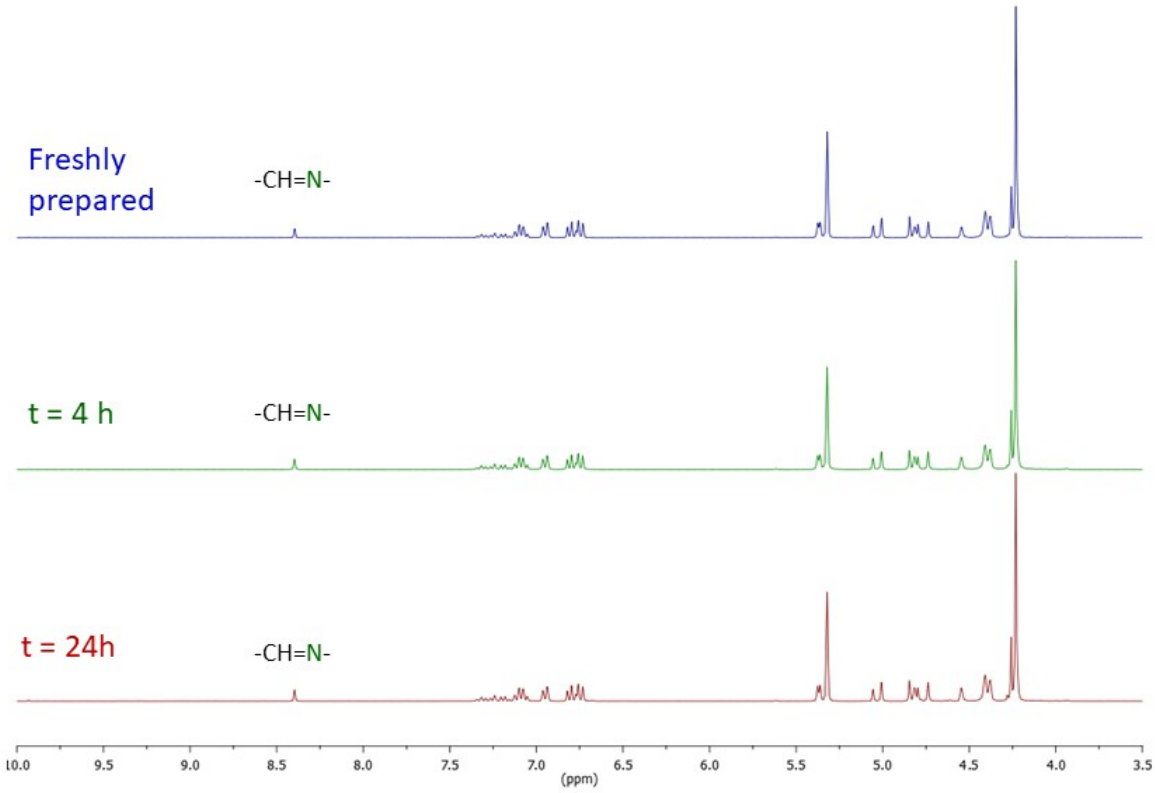

(B)

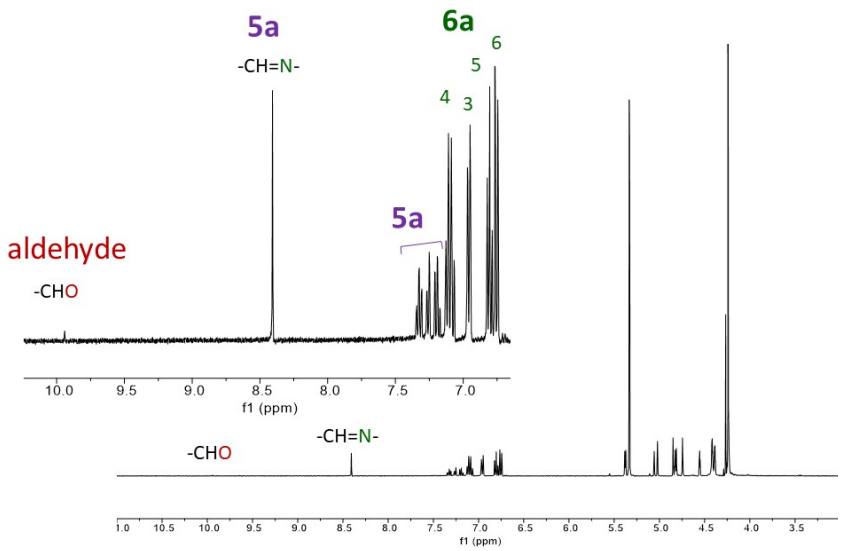

Figure S20. (**A**) ^{1}H-NMR spectrum of a freshly prepared solution of compound **6b** in CD_2Cl_2 at 298 and after different periods of storage (t = 4h, 24 h) at 298 K. (**B**) ^{1}H-NMR spectrum of the same sample after 30 h of storage at 298 K and an expansion showing the presence of **5b**, **6b** and benzaldehyde.

(A)

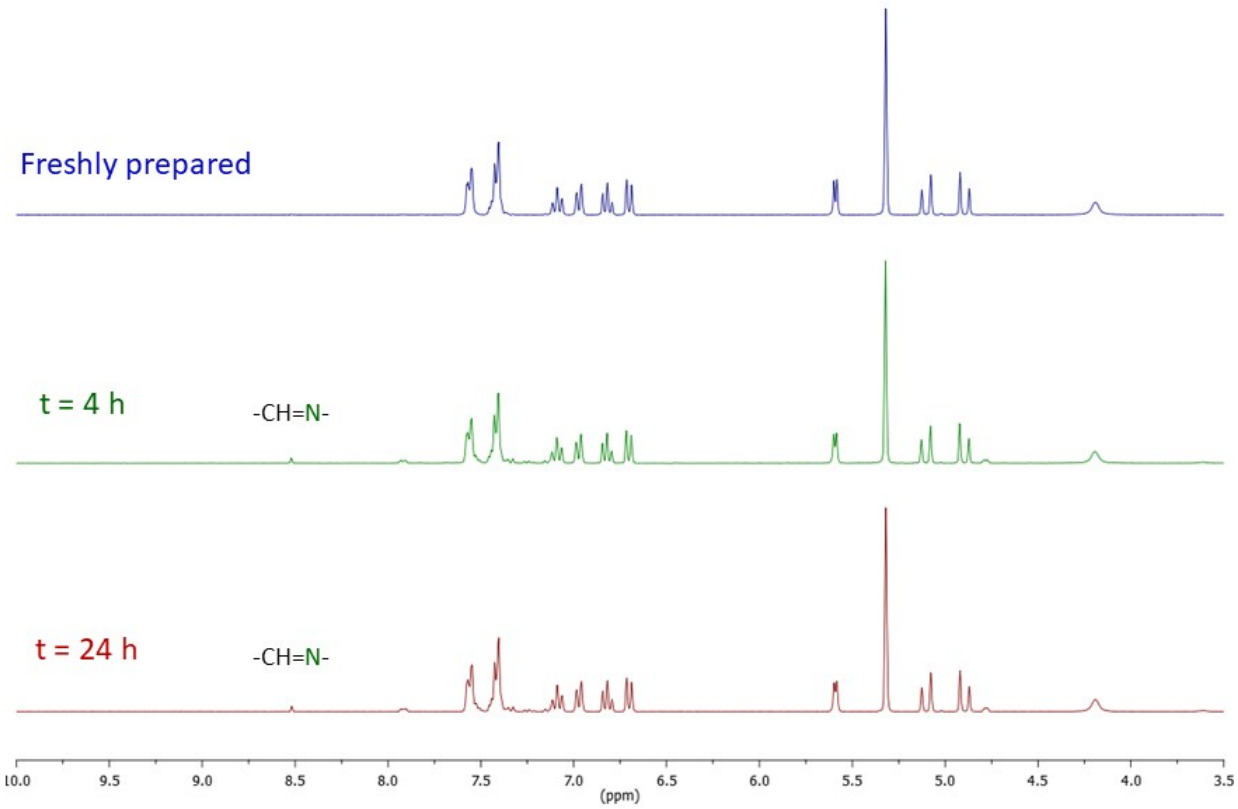

(B)

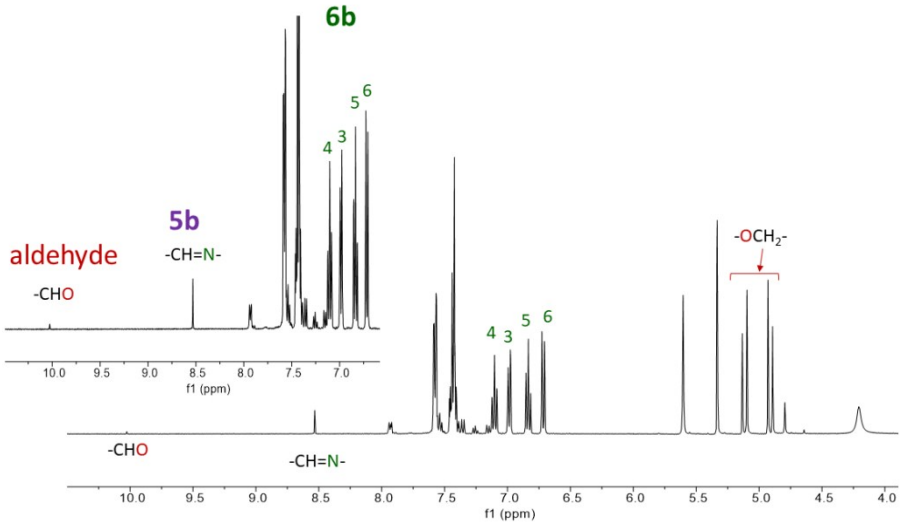

Figure S21. ^{1}H-NMR spectrum of compound **6c** (in benzene-d_6 at 298 K). Expansions of selected regions of the spectrum are shown as insets together with the assignment of the resonances.

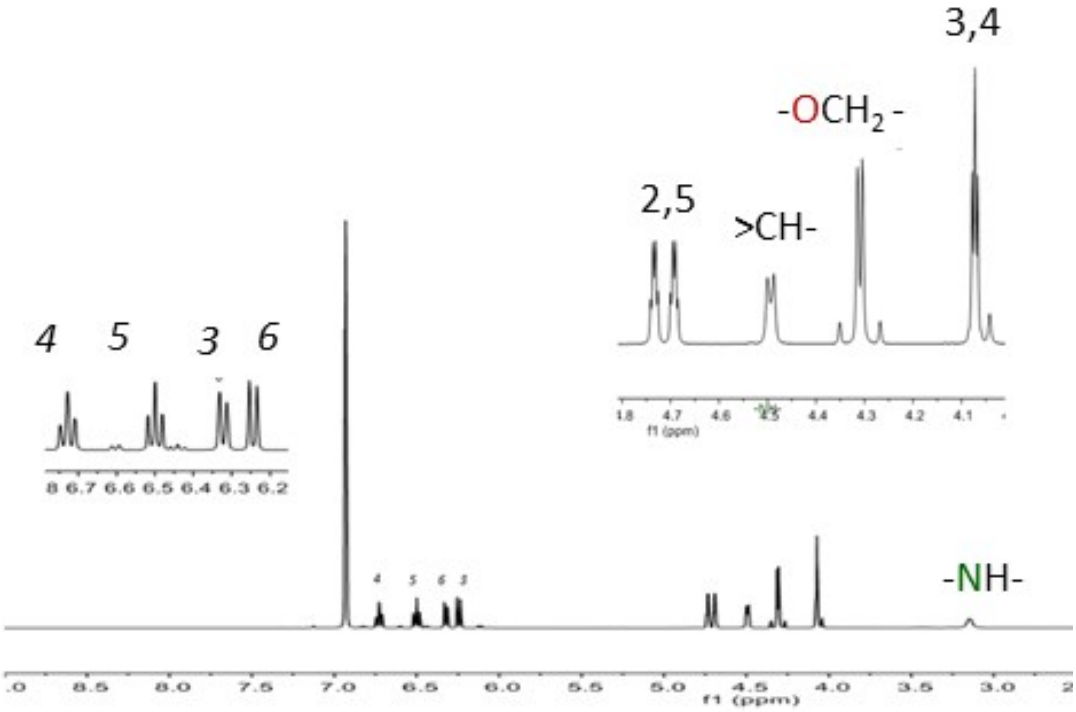

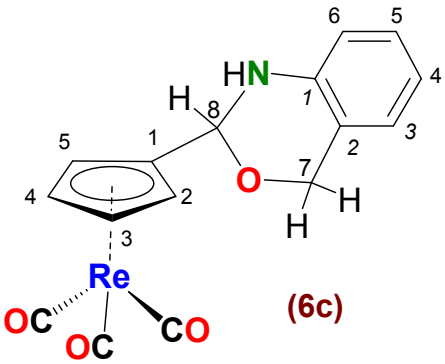

Figure S22. ^{1}H-NMR spectrum of compound **6d** (in benzene-d_6 at 298 K). Expansions of selected regions of the spectrum are shown as insets together with the assignment of the resonances.

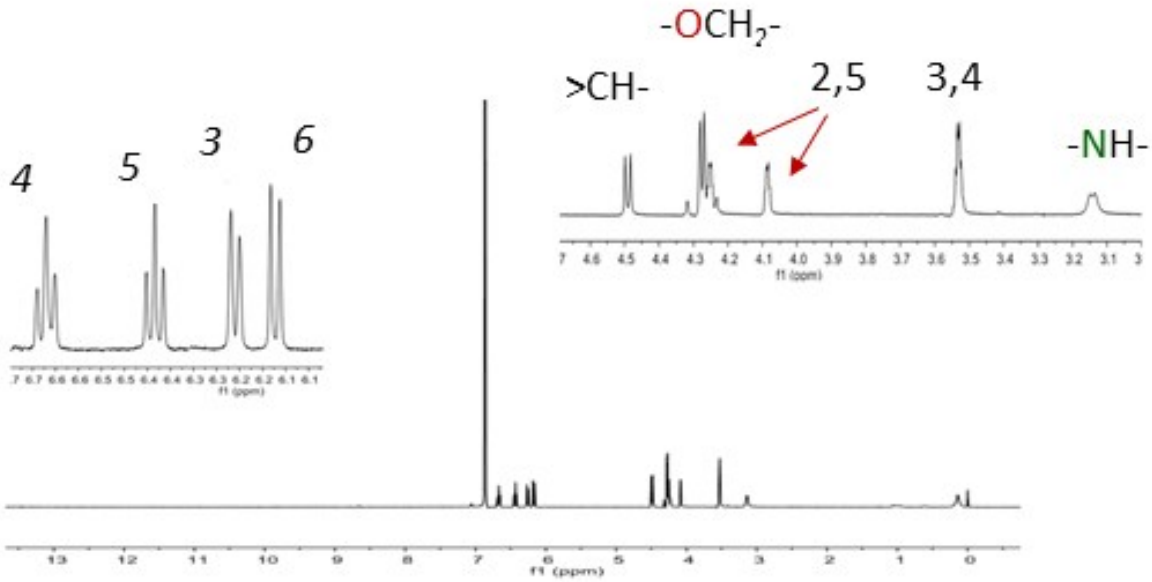

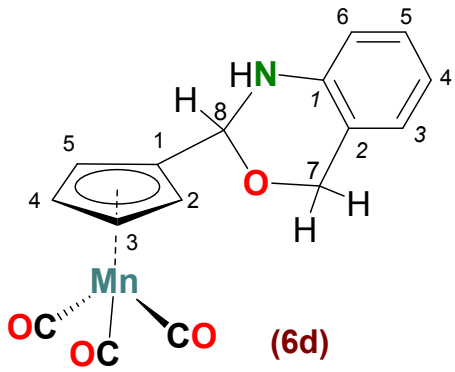

(6d)

Figure S23. $^{13}C\{^{1}H\}$-NMR spectra of compound **6c** (**A**) in CD_2Cl_2 and (**B**) in benzene-d_6 at 298 K.

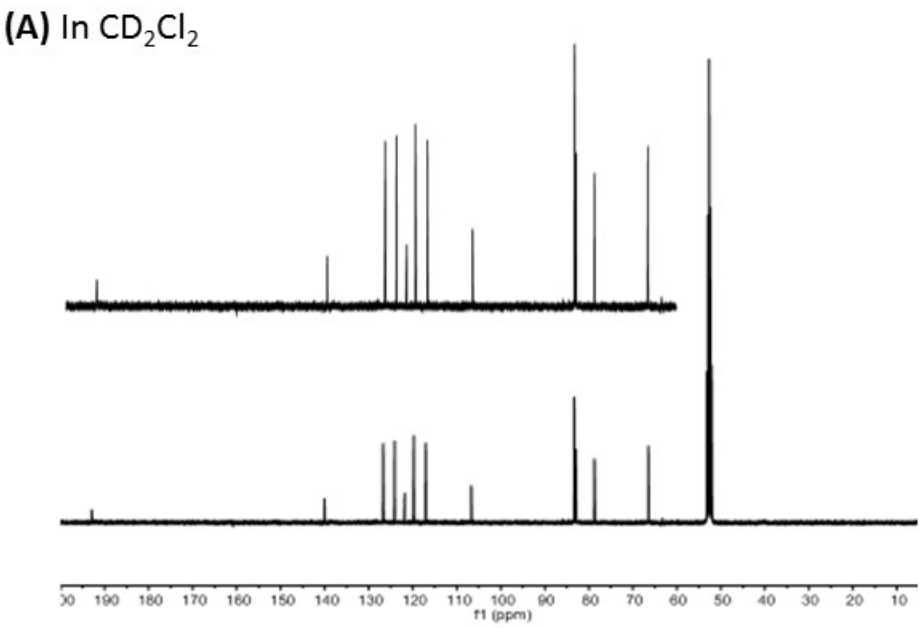

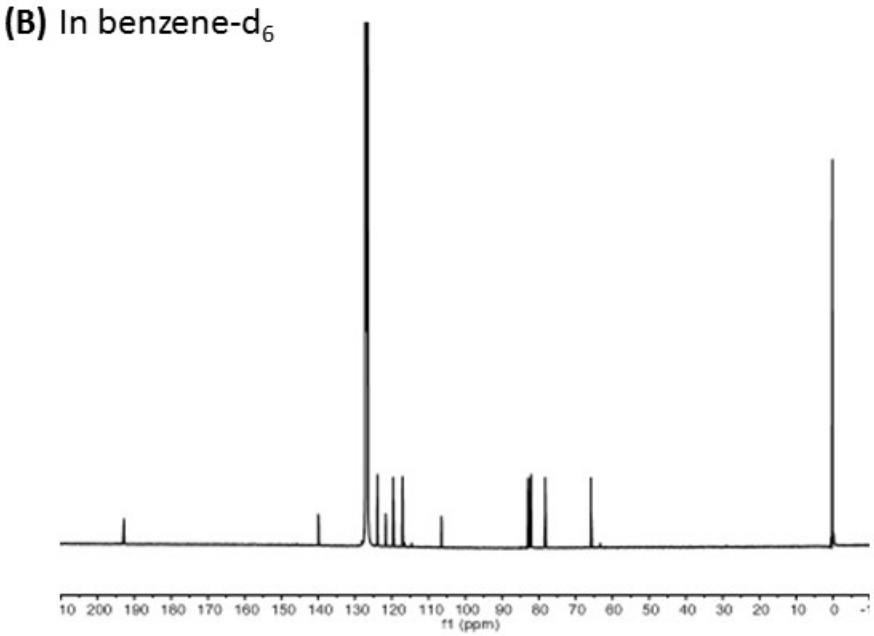

Figure S24. $^{13}C\{^{1}H\}$ -NMR spectra of compound **6d** (**A**) in CD_2Cl_2 and (**B**) in benzene-d_6 at 298 K.

(**A**) In CD_2Cl_2

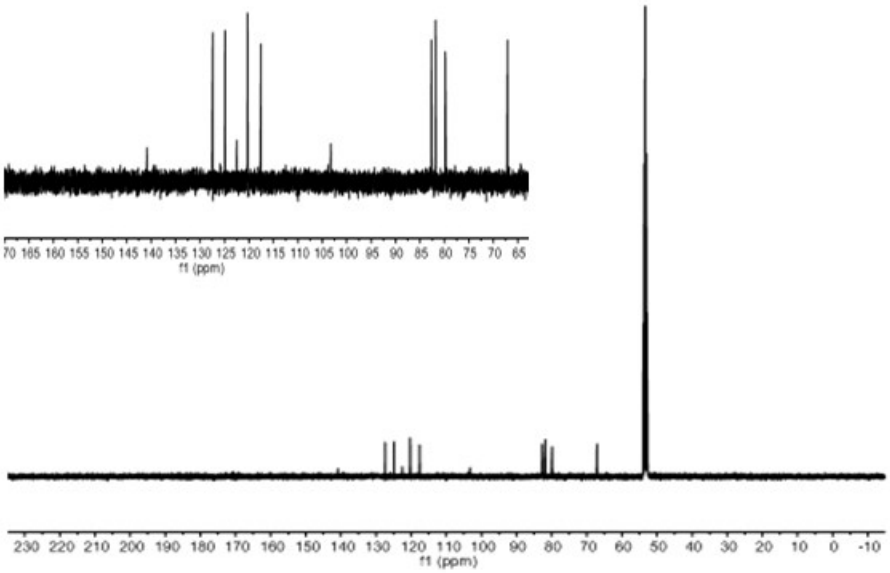

(**B**) In benzene-d_6

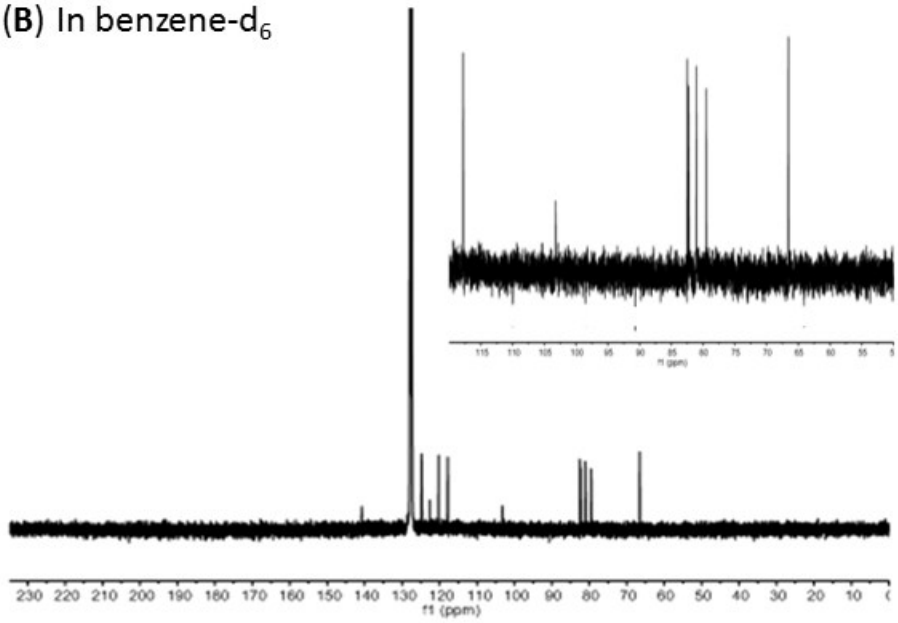

Figure S25. ^{1}H-NMR spectrum of a freshly prepared solution of compound **6c** in DMSO-d_6 at 298 and after different periods of storage (*t*). For *t* = 10 months the spectra showed additional resonances (marked with a yellow arrow) that indicate the presence of a minor component.

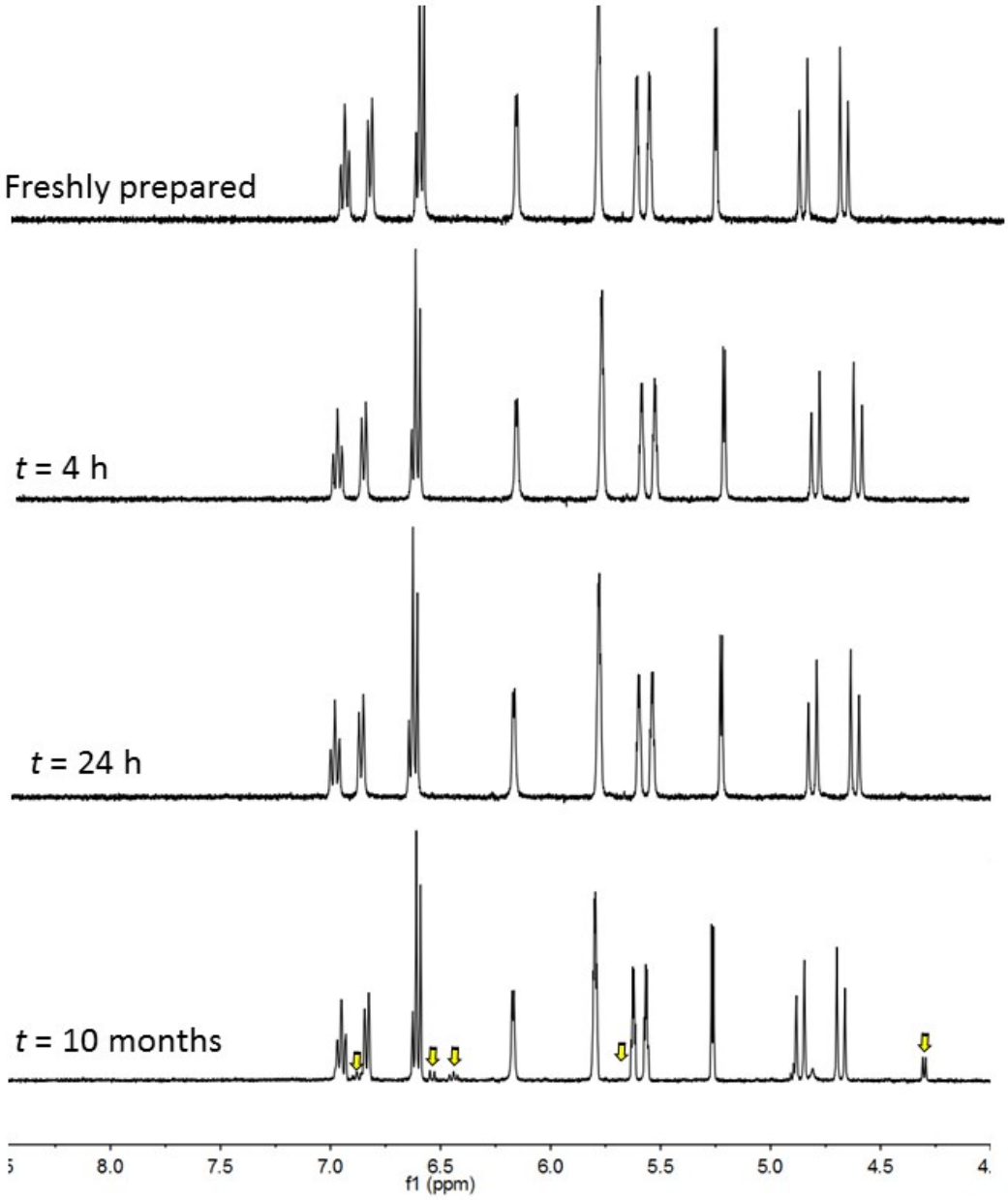

Figure S26. ^{1}H-NMR spectrum of a freshly prepared solution of compound **6d** in DMSO-d_6 at 298 K and after different periods of storage (*t*).

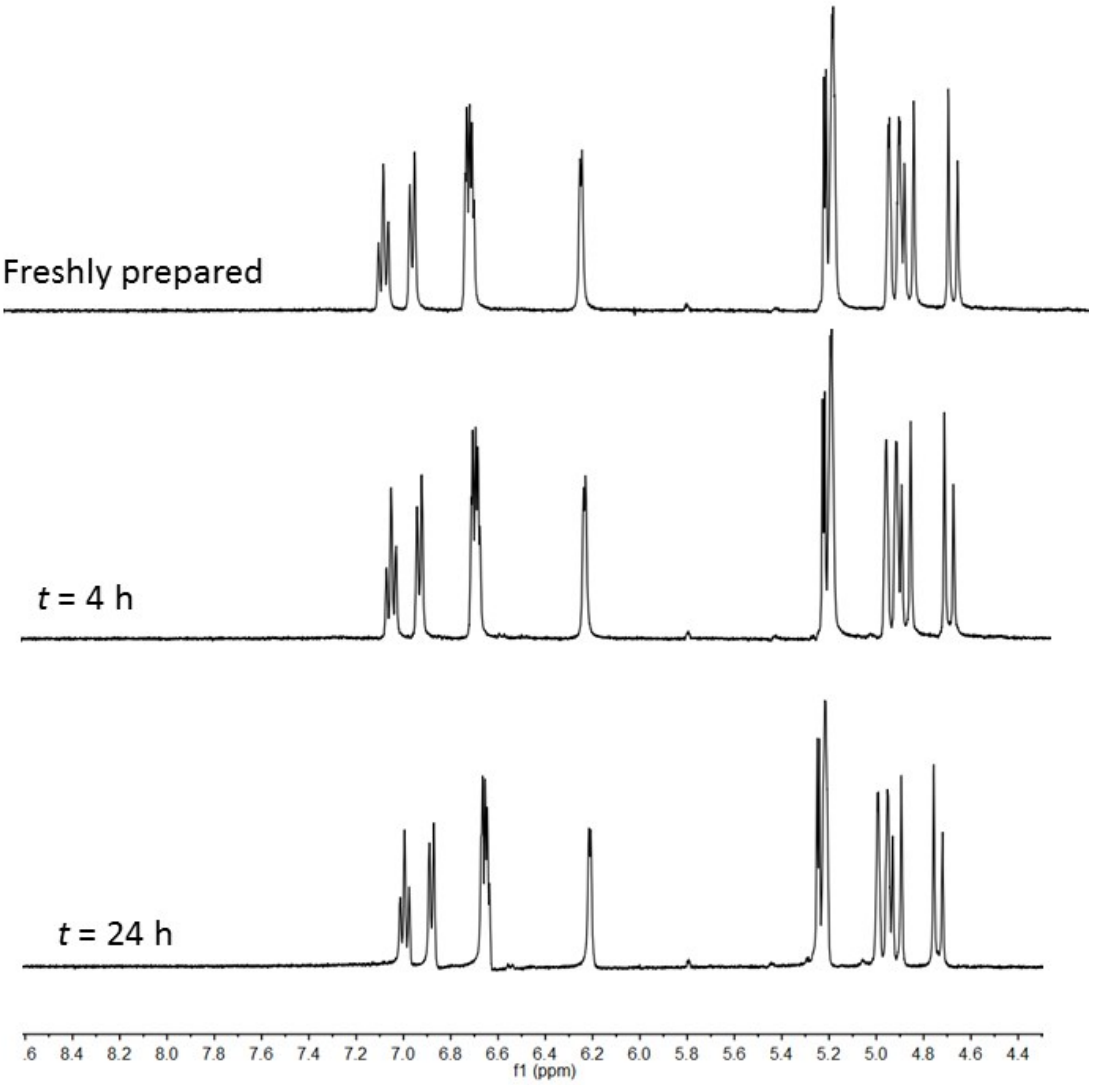

Figure S27. ^{1}H (top) and $^{13}C\{^{1}H\}$ (bottom) NMR spectra (300 MHz) of the aldimine $[Re\{(\eta^5\text{-}C_5H_4)\text{-}CH{=}N\text{-}(C_6H_4\text{-}2\text{-}OH)\}(CO)_3]$ (**7c**) in $CDCl_3$ at 298.

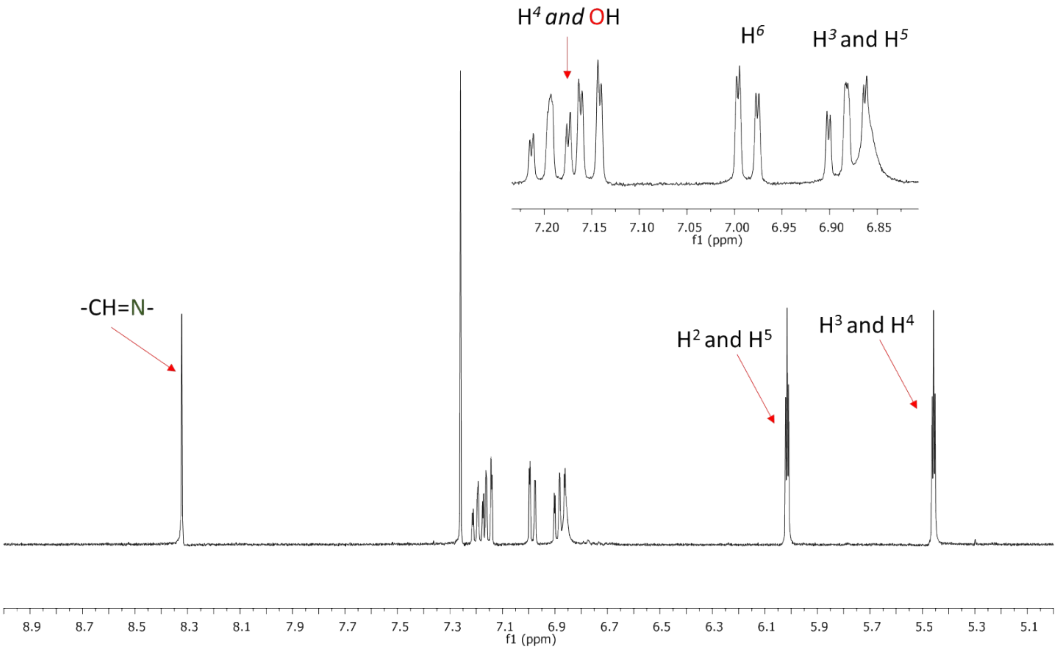

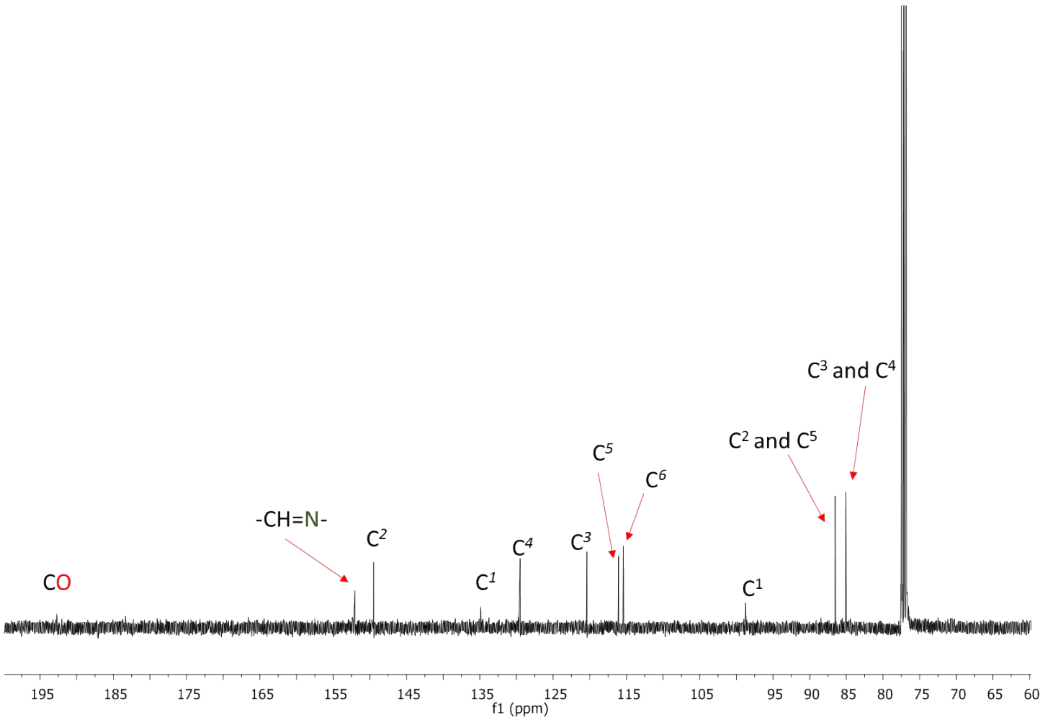

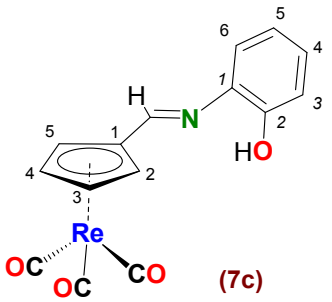

Figure S28. ^{1}H-NMR spectra (300 MHz) of the aldimine [Mn{(η^5-C_5H_4)-CH=N-(C_6H_4-2-OH)}$(CO)_3$] (**7d**) in $CDCl_3$ at 298 K.

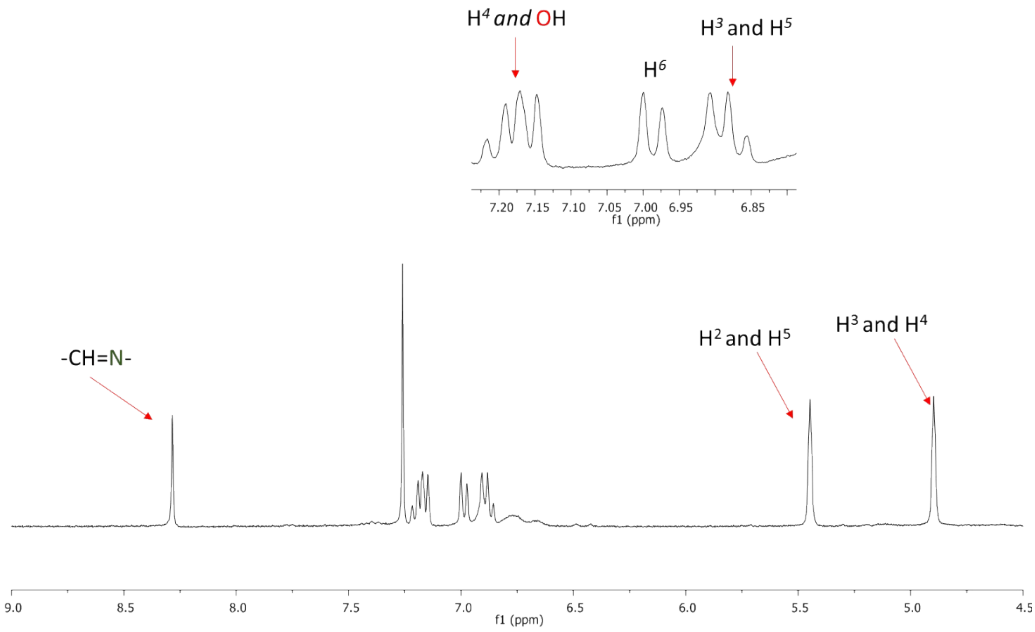

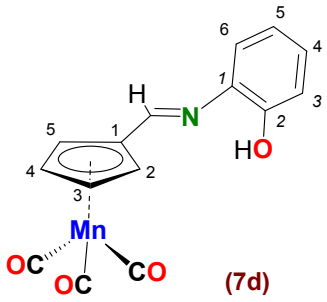

Figure S29. ^{1}H-NMR spectra (300 MHz) of a freshly prepared solution of the aldimine [Re{(η^5-C_5H_4)-CH=N-(C_6H_4-2-OH)}$(CO)_3$] (**7c**) in DMSO-d_6 at 298 K and after different periods of storage (*t*).

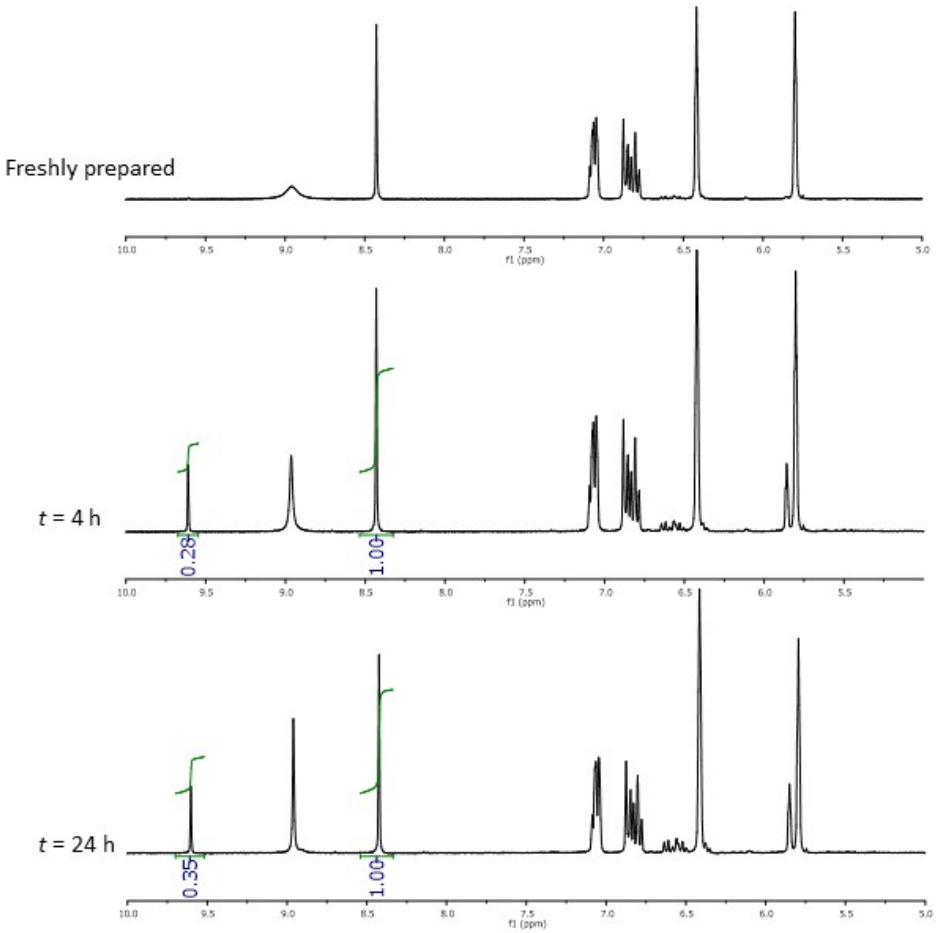

Figure S30. ^{1}H-NMR spectra (300 MHz) of a freshly prepared solution of the aldimine [Re{(η^5-C_5H_4)-CH=N-(C_6H_4-2-OH)}$(CO)_3$] (**7d**) in DMSO-d_6 at 298 K and after different periods of storage (*t*).

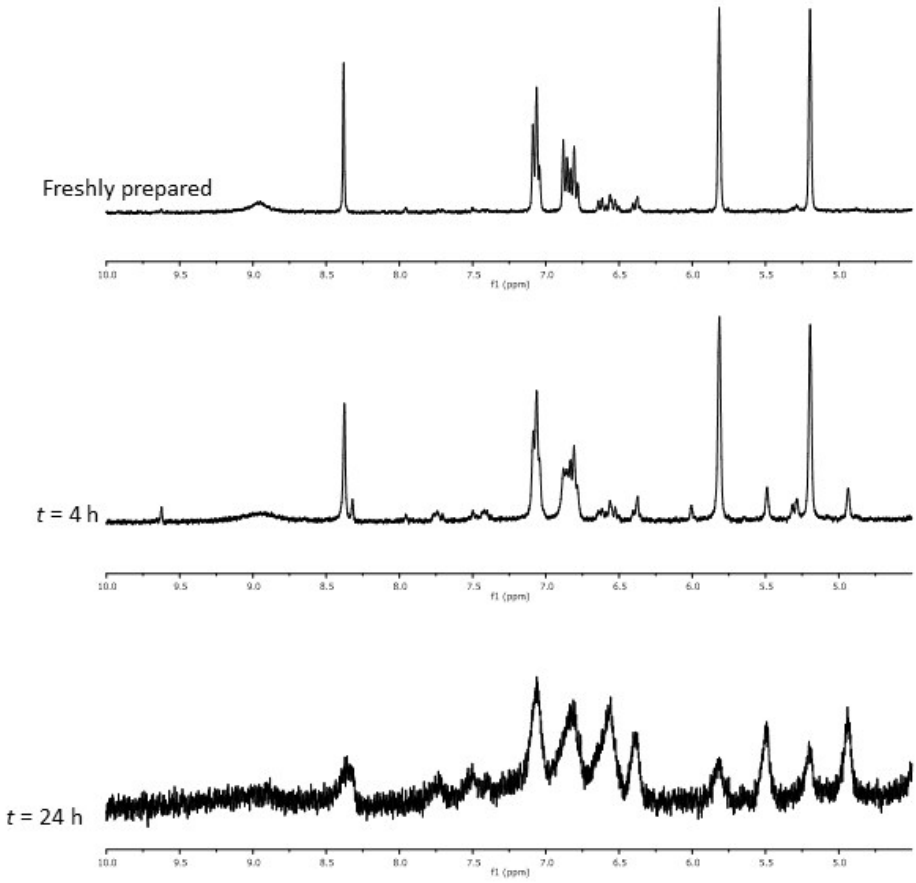

Figure S31. UV-visible spectra of CH_2Cl_2 solutions of the 2-R-2,4-dihydro-1*H*-3,1-benzoxazines under study [R = ferrocenyl (**6a**), phenyl (**6b**) cyrhetrenyl (**6c**) and cymantrenyl (**6d**)] at 298 K.

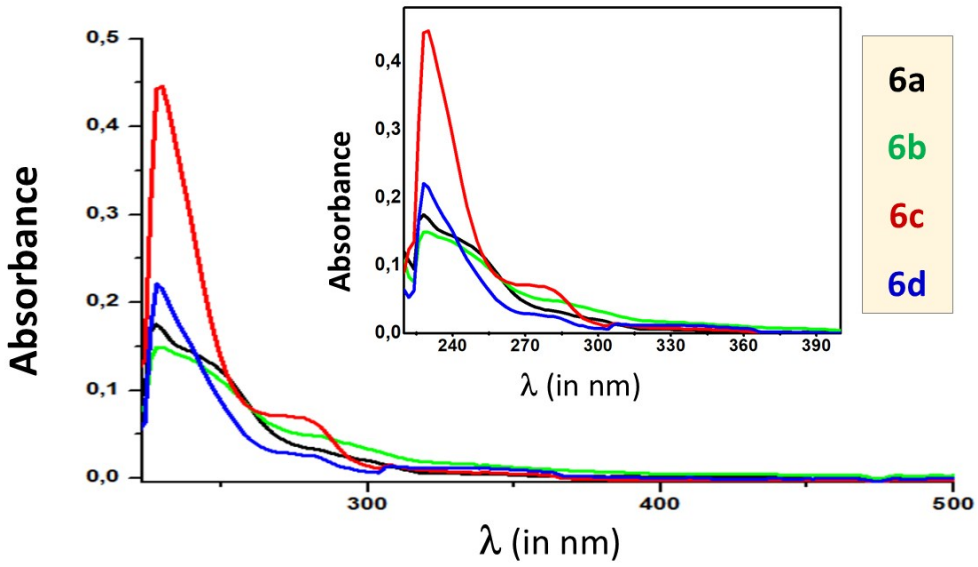

2.-SUPPLEMENTARY TABLES

Table S1. Crystal data and details of the refinement of the crystal structures of the 2-ferrocenyl, 2,4-dihydro-1*H*-3,1-benzoxazine (**6a**) and its 2-cyrhetrenyl- or 2-cymantrenyl- analogues (**6c** and **6d,** respectively).

	6a	**6c**	**6d**
Crystal size[a]	0.10 × 0.06 × 0.05	0.332 × 0.041 × 0.031	0.399 × 0.154 × 0.046
Empirical formula	$C_{18}H_{17}FeNO_4$	$C_{16}H_{12}ReNO_4$	$C_{16}H_{12}MnNO_4$
Formula weight	319.17(2)	468.47(2)	337.21(2)
Temperature (K)	170(2)	100(2)	100(2)
λ (nm)	0.71073	0.71073	0.71073
Crystal system	Monoclinic	Orthorhombic	Monoclinic
Space group	$P2_1$	$Pna2_1$	C2/c
a (Å)	5.9213(2)	15.3555(7)	30.935(3)
b (Å)	7.5337(3)	6.1536(3)	6.1805(5)
c (Å)	16.2535(7)	29.7559(13)	15.1240(14)
$\alpha = \gamma$ (deg.)	90	90	90
β (deg.)	96.7714(15)	90	108.124(4)
V (Å^3)	720.00(5)	2811.7(2)	2748.1(4)
Z	2	8	8
$D_{calc.}$ (Mg × m^{-3})	1.472	2.213	1.630
μ(mm^{-1})	1.044	8.661	0.978
F(000)	332	1776	1376
Θ range for data collect. (deg.)	from 2.524 to 26.416	from 2.653 to 29.554	from 2.740 to 30.174
Index ranges	$-7 \le h \le 7$	$-21 \le h \le 19$	$-43 \le h \le 43$
	$-9 \le k \le 9$	$-8 \le k \le 6$	$-8 \le k \le 8$
	$-20 \le l \le 20$	$-35 \le l \le 41$	$-21 \le l \le 21$
N. of collected reflect.	16003	25066	35346
N. independent reflect. [R_{int}]	2941[0.0258]	7511[0.0402]	4058[0.0907]
Completeness to Θ = 25.242	99.6 %	99.7 %	99.4 %
Absorption correct.	← Semi-empirical from equivalents →		
Refinement method	← Full matrix least squares on F^2 →		
N. of data	2941	7509	4058
N. of parameters	165	386	199
Goodness of fit on F^2	1.068	1.227	1.060
Final R indices [$I > 2\sigma(I)$]	R_1 = 0.0228,	R_1 = 0.0359,	R_1 = 0.0458,
	wR_2 = 0.0569	wR_2 = 0.0791	wR_2 = 0.1183

Final R indices (all data)	R_1 = 0.0247, wR_2 = 0.0545	R_1 = 0.0439, wR_2 = 0.0822	R_1 = 0.0609, wR_2 = 0.1227
Absolute structure parameter	0.023(18)	0.269(16)	n/a

[a] (mm × mm × mm).

Table S2. Final atomic coordinates for the optimized geometry of imine R-CH=N-(C_6H_4-2-CH_2OH), [with R = (η^5-C_5H_5)Fe(η^5-C_5H_4), (**5a**)].

H	-3.48236	-0.71380	-2.40508
C	-2.76596	-1.07418	-1.67869
C	-3.06565	-1.88651	-0.54133
H	-0.84205	-0.15744	-2.37024
H	-4.04486	-2.25014	-0.25971
C	-1.85907	-2.09316	0.18189
H	-1.75333	-2.64539	1.10707
C	-0.79822	-1.41044	-0.51019
C	-1.37761	-0.77158	-1.66016
C	0.57040	-1.29209	-0.03570
H	0.78804	-1.78063	0.92431
N	1.46623	-0.62195	-0.66754
C	2.77366	-0.50302	-0.14658
C	5.36931	-0.16693	0.86658
C	3.46015	0.71316	-0.37070
C	3.41386	-1.54447	0.54624
C	4.70320	-1.37920	1.04848
C	4.74391	0.86255	0.16020
H	2.90803	-2.49944	0.65838
H	5.18596	-2.19804	1.57521
H	5.26787	1.80386	0.00797
H	6.37155	-0.02570	1.26154
C	2.86861	1.81868	-1.23424
H	3.05780	1.56731	-2.29287
H	3.39782	2.75582	-1.03305
O	1.48799	2.07997	-1.03487
H	1.05501	1.21545	-1.17649
Fe	-2.26188	-0.05800	0.08406
H	-2.77926	2.53273	-0.94032
C	-2.67822	1.98210	-0.01428
C	-1.46280	1.77007	0.70192
H	-4.76246	1.24464	0.36454
H	-0.47972	2.11977	0.41105
C	-1.76130	0.95089	1.83400
H	-1.04480	0.58674	2.55865
C	-3.15933	0.66260	1.81933
H	-3.68954	0.03955	2.52774
C	-3.72700	1.29929	0.67449

Table S3. Final atomic coordinates for the optimized geometry of imine R-CH=N-(C_6H_4-2-CH_2OH)] (R = Ph, **5b**).

C	0.69016	-0.74089	0.15811
H	0.46054	-1.70173	0.64031
N	-0.23908	0.04371	-0.25235
C	-1.59613	-0.33462	-0.17395
C	-4.32488	-0.96691	-0.03249
C	-2.54937	0.70121	-0.04178
C	-2.02791	-1.66773	-0.27609
C	-3.38344	-1.98175	-0.20484
C	-3.90047	0.36125	0.04497
H	-1.30115	-2.45612	-0.45000
H	-3.70221	-3.01694	-0.29288
H	-4.63458	1.15467	0.16602
H	-5.38324	-1.20504	0.02813
C	-2.11385	2.15656	-0.03745
H	-2.97626	2.79144	0.18927
H	-1.77097	2.42411	-1.05129
O	-1.12117	2.47234	0.92623
H	-0.34453	1.94783	0.66360
C	2.11556	-0.41920	0.04220
C	4.85685	0.14084	-0.13530
C	3.06054	-1.29234	0.60475
C	2.56314	0.73957	-0.61811
C	3.92303	1.01577	-0.70278
C	4.42348	-1.01419	0.51782
H	2.71982	-2.19082	1.11463
H	1.82964	1.40569	-1.06094
H	4.26118	1.91291	-1.21408
H	5.14542	-1.69596	0.95865
H	5.91890	0.35992	-0.20518

Table S4. Final atomic coordinates for the optimized geometry of the R-CH=N-(C_6H_4-2-CH_2OH) (R = Re(η^5-C_5H_4)$(CO)_3$, **5c**).

Re	1.91464	0.04907	0.02861
H	2.28979	-3.00522	0.07690
C	1.68457	-2.26254	-0.42519
C	2.01545	-1.59800	-1.65865
H	-0.10612	-2.09167	0.90141
H	2.90266	-1.76305	-2.25423
C	0.95113	-0.71049	-1.96904
H	0.88966	-0.07490	-2.84328
C	-0.05969	-0.82297	-0.94886
C	0.42429	-1.78369	0.01113
C	2.16401	1.85030	-0.59592
O	2.27983	2.92020	-1.03017
C	3.74283	-0.01955	0.61525
O	4.85220	-0.12191	0.93870
C	1.35984	0.70037	1.75503
O	0.97845	1.05150	2.79147
C	-1.34659	-0.13614	-0.94660
H	-1.46453	0.66717	-1.68600
N	-2.29440	-0.46808	-0.14964
C	-3.50398	0.26348	-0.13849
C	-5.93893	1.64194	-0.05815
C	-4.70391	-0.45564	0.06839
C	-3.53453	1.66093	-0.26710
C	-4.74774	2.34705	-0.22910
C	-5.90611	0.25312	0.09415
H	-2.60127	2.21044	-0.35509
H	-4.75771	3.42990	-0.31745
H	-6.83423	-0.29302	0.24604
H	-6.88752	2.17021	-0.02068
C	-4.68154	-1.96843	0.21447
H	-4.44922	-2.42262	-0.76541
H	-5.67818	-2.32103	0.49879
O	-3.78851	-2.43067	1.21292
H	-2.93110	-2.02160	0.98964

Table S5. Final atomic coordinates for the optimized geometry of the R-CH=N-(C_6H_4-2-CH_2OH) (R = Mn(η^5-C_5H_4)$(CO)_3$, **5d**).

H	3.05263	-2.77251	-0.14679
C	2.41851	-2.01490	-0.58755
C	2.76112	-1.17182	-1.69671
H	0.56971	-2.12711	0.65614
H	3.69110	-1.18945	-2.24839
C	1.65780	-0.32208	-1.94814
H	1.59983	0.43065	-2.72421
C	0.62021	-0.62200	-1.00280
C	1.11465	-1.67745	-0.16203
C	2.52712	1.82983	-0.33335
O	2.58970	2.94637	-0.62429
C	4.08666	-0.00124	0.66131
O	5.17975	-0.09223	1.02332
C	1.72006	0.39870	1.69384
O	1.25796	0.57673	2.73580
C	-0.69224	0.01007	-0.95579
H	-0.83506	0.87144	-1.62258
N	-1.63507	-0.42286	-0.20222
C	-2.87322	0.25657	-0.14360
C	-5.36557	1.52147	0.02673
C	-4.04158	-0.52489	0.01180
C	-2.96419	1.65702	-0.17541
C	-4.20550	2.28656	-0.09337
C	-5.27309	0.12834	0.08415
H	-2.05591	2.25142	-0.22427
H	-4.26173	3.37156	-0.10762
H	-6.17669	-0.46615	0.19761
H	-6.33576	2.00508	0.09865
C	-3.95457	-2.04182	0.05853
H	-3.70201	-2.42128	-0.94773
H	-4.93557	-2.45421	0.31571
O	-3.04339	-2.52923	1.02826
H	-2.20453	-2.07010	0.83326
Mn	2.39801	0.08173	0.05622

Table S6. Final atomic coordinates for the optimized geometry of the 2-ferrocenyl 2,4-dihydro-1*H*-3,1-benzoxazine (**6a**).

H	3.75763	-2.32938	0.23641
C	2.80371	-1.94817	-0.10356
C	2.51116	-1.46605	-1.41594
H	3.20492	-1.42000	-2.24508
C	1.15998	-1.01503	-1.43159
H	0.63494	-0.57731	-2.26895
C	0.61466	-1.20308	-0.12247
C	1.63322	-1.78930	0.69395
C	-0.78995	-0.91239	0.30956
H	-0.80843	-0.72921	1.40227
N	-1.34030	0.22114	-0.42104
H	-0.74011	1.03666	-0.42197
H	1.53571	-2.03840	1.74274
O	-1.59659	-2.04930	0.04235
C	-2.91101	-1.90494	0.57383
H	-2.89049	-2.05679	1.66763
H	-3.49138	-2.72671	0.14168
C	-3.53259	-0.56442	0.23507
C	-4.63379	1.93327	-0.39517
C	-4.89957	-0.32863	0.38835
C	-2.70333	0.47119	-0.24018
C	-3.26798	1.71731	-0.55716
C	-5.46030	0.91180	0.08105
H	-5.53602	-1.13328	0.75291
H	-2.62710	2.51138	-0.93521
H	-6.52644	1.07723	0.20501
H	-5.05369	2.90456	-0.64353
Fe	2.25953	0.05867	-0.01697
H	4.17847	1.60098	-1.41569
C	3.54569	1.60791	-0.53794
C	3.89030	1.09562	0.74921
H	1.64806	2.52350	-1.29871
H	4.83013	0.63138	1.01739
C	2.76126	1.25878	1.60733
H	2.69627	0.94668	2.64132
C	1.71895	1.87521	0.85065
H	0.73271	2.12387	1.22178
C	2.20323	2.09025	-0.47673

Table S7. Final atomic coordinates for the optimized geometry of 2-phenyl 2,4-dihydro-1*H*-3,1-benzoxazine (**6b**).

C	-0.46220	0.29117	0.48201
H	-0.29263	0.36879	1.56953
N	0.33610	-0.83007	0.01554
H	-0.04009	-1.23942	-0.83570
O	-0.05463	1.52556	-0.10354
C	1.25802	1.86471	0.32699
H	1.23343	2.19588	1.38033
H	1.55863	2.72479	-0.28002
C	2.23032	0.71572	0.14217
C	3.98784	-1.40700	-0.36172
C	3.61283	0.92443	0.12467
C	1.72901	-0.58111	-0.06185
C	2.61607	-1.63525	-0.32533
C	4.49470	-0.12562	-0.12159
H	3.99962	1.92989	0.28241
H	2.21457	-2.63314	-0.48345
H	5.56599	0.05348	-0.13812
H	4.66491	-2.23238	-0.56532
C	-1.93336	0.05436	0.20591
C	-4.65875	-0.41553	-0.25872
C	-2.72606	1.03799	-0.39324
C	-2.51595	-1.16582	0.57533
C	-3.87130	-1.39908	0.34395
C	-4.08246	0.80116	-0.62532
H	-2.27366	1.98183	-0.67470
H	-1.90232	-1.93038	1.04374
H	-4.31231	-2.34875	0.63541
H	-4.68911	1.57126	-1.09474
H	-5.71506	-0.59667	-0.43932

Table S8. Final atomic coordinates for the optimized geometry of the 2-cyrhetrenyl 2,4-dihydro-1*H*-3,1-benzoxazine (**6c**).

Re	1.79390	0.09466	0.00599
H	2.88684	-2.77861	0.01397
C	1.98688	-2.24119	-0.25176
C	1.67983	-1.68303	-1.54227
H	2.31407	-1.72046	-2.41766
C	0.38944	-1.09707	-1.47136
H	-0.14141	-0.60482	-2.27437
C	-0.11705	-1.26461	-0.13698
C	0.87827	-1.98601	0.60127
C	1.95385	0.69659	1.82525
O	2.01845	1.00096	2.94368
C	1.17386	1.82508	-0.54538
O	0.72688	2.83579	-0.90722
C	3.61975	0.59972	-0.34491
O	4.72726	0.84629	-0.58666
C	-1.51578	-0.96165	0.32289
H	-1.53336	-0.88241	1.42723
N	-2.02740	0.24490	-0.31128
H	-1.44683	1.06165	-0.15657
H	0.79368	-2.28804	1.63737
O	-2.32769	-2.05734	-0.06219
C	-3.65913	-1.94569	0.44103
H	-3.66854	-2.17875	1.51989
H	-4.22645	-2.73091	-0.06865
C	-4.25834	-0.58037	0.18065
C	-5.31365	1.97043	-0.28758
C	-5.63087	-0.34710	0.28739
C	-3.40384	0.48194	-0.16739
C	-3.94318	1.75596	-0.40347
C	-6.16790	0.91980	0.05957
H	-6.28807	-1.17328	0.55306
H	-3.27952	2.57168	-0.68182
H	-7.23778	1.08455	0.14574
H	-5.71559	2.96322	-0.47126

Table S9. Final atomic coordinates for the optimized geometry of the open form 2-cymanentryl 2,4-dihydro-1H-3,1-benzoxazine (**6d**).

Mn	2.06700	0.14318	-0.14300
H	2.78868	-2.15413	-1.80924
C	1.93108	-1.63429	-1.40382
C	1.22095	-0.55713	-2.02785
H	1.45013	-0.11513	-2.98831
C	0.16607	-0.17032	-1.16527
H	-0.54651	0.62210	-1.35026
C	0.21514	-0.98563	0.01370
C	1.30257	-1.89878	-0.16091
C	2.94634	-0.20973	1.38018
O	3.49240	-0.47705	2.36337
C	1.51148	1.74124	0.43427
O	1.08793	2.75234	0.80905
C	3.52920	0.81169	-0.94496
O	4.46031	1.21687	-1.49620
C	-0.76810	-1.01649	1.17408
H	-0.21594	-1.22236	2.09607
N	-1.51311	0.21740	1.35972
H	-0.96610	1.03086	1.60977
H	1.60414	-2.65405	0.55391
O	-1.67310	-2.09896	1.05297
C	-2.57059	-1.98406	-0.05366
H	-3.30619	-2.78060	0.09454
H	-2.03554	-2.20164	-0.99309
C	-3.23741	-0.62864	-0.11445
C	-4.38999	1.91940	-0.24336
C	-4.39967	-0.40927	-0.85492
C	-2.64653	0.44617	0.57969
C	-3.23489	1.72054	0.50808
C	-4.98276	0.85618	-0.93040
H	-4.85346	-1.24643	-1.38262
H	-2.78224	2.54797	1.05017
H	-5.88721	1.00954	-1.51130
H	-4.83057	2.91187	-0.28851

Table S10. Calculated distances between the imine nitrogen and atoms of the pendant –OH moiety in the imines R-CH=N-(C_6H_4-2-CH_2OH) **5a-5d**, the Mulliken charges on the atoms involved in the 6-endo trig process and differences between their Mulliken charges.

	compound			
	5a	**5b**	**5c**	**5d**
R =	ferrocenyl	phenyl	cyrhetrenyl	cymantrenyl
O-H	0.977	0.973	0.976	0.976
N····H	1.950	2.116	2.023	2.027
N····O	2.727	2.840	2.817	2.817
Mulliken charges				
O	-0.648	-0.627	-0.649	-0.649
C_{imine}	+0.047	+0.041	+0.031	+0.025
N	-0.466	-0.522	-0.444	-0.446
Charge differences				
$q_{C(imine)} - q_O$	0.695	0.668	0.680	0.674
$q_{C(imine)} - q_N$	0.563	0.513	0.475	0.471

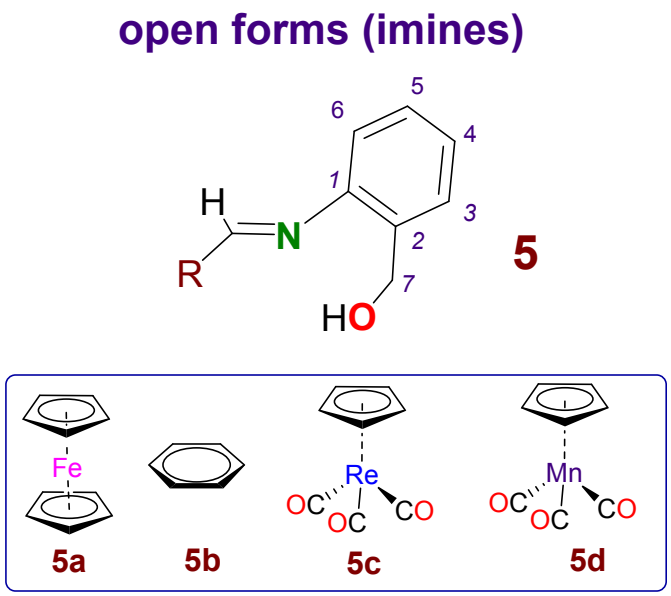

Table S11. A) Calculated electronic energies (*E* in hartrees) for the imine forms R-CH=N-(C_6H_4-2-CH_2OH) (**5a-5d**) and their corresponding: 2-R-2,4-dihydro-1*H*-3,1-benzoxazines (**6a-6d**) in vacuum and in CH_2Cl_2, and free energy (*G*) calculated for both tautomers at 25 °C under identical experimental conditions; **B)** Differences between the electronic energies (ΔE) and free energies (ΔG) (in kcal /mol) of the imine forms R-CH=N-(C_6H_4-2-CH_2OH) (**5a-5d**) and those obtained for their corresponding tautomers 2-R-2,4-dihydro-1*H*-3,1 benzoxazines (**6a-6d**), with the same R group, under identical conditions in vacuum and in CH_2Cl_2 and the calculated values of the free energy of the reactions $\boldsymbol{6}_i \rightarrow \boldsymbol{5}_i$

A)

		Electronic energy, *(E)*				**Free energy** (*G*)			
		In vacuum		In CH_2Cl_2		In vacuum		In CH_2Cl_2	
R	**i**	**5**	**6**	**5**	**6**	**5**	**6**	**5**	**6**
Ferrocenyl	**a**	-949.532073	-949.53894	-949.546184	-949.552863	-949.271199	-949.276525	-949.28531	-949.290448
Phenyl	**b**	-671.274740	-671.284638	-671.290487	-671.297026	-671.080003	-671.08453	-671.09575	-671.096918
Cyrhenetryl	**c**	-1051.74750	-1051.75822	-1051.76519	-1051.77357	-1051.55389	-1051.56063	-1051.57157	-1051.57597
Cymantrenyl	**d**	-1076.51436	-1076.52391	-1076.532021	-1076.53793	-1076.32023	-1076.32412	-1076.33608	-1076.33814

B)

R and identification letter		$\Delta E = E$(for **5**$_i$) - E(for **6**$_i$)		$\Delta G = G$(for **5**$_i$)-G(for **6**$_i$)		ΔG for the reaction ***6***$_i \rightarrow$ ***5***$_i$
R	**i**	in vacuum	In CH_2Cl_2	in vacuum	In CH_2Cl_2	at 298 K, in CH_2Cl_2
Ferrocenyl	**a**	4.31	4.19	3.34	1.29	-3.22
Phenyl	**b**	6.21	4.10	2.84	0.73	-0.73
Cyrhenetryl	**c**	6.73	5.26	4.23	2.76	-2.76
Cymantrenyl	**d**	5.99	4.84	2.44	1.29	-1.29

Table S12. Calculated energy (in eV) of the HOMO and LUMO orbitals [$E_{(HOMO)}$ and $E_{(LUMO)}$, respectively] and the energy gap [$E_{gap} = E_{(LUMO)} - E_{(HOMO)}$ (in eV)] for the closed forms **6a-6d**, shown below and Mulliken charges on selected atoms.

	compound			
	6a	**6b**	**6c**	**6d**
R =	ferrocenyl	phenyl	cyrhetrenyl	cymantrenyl
$E_{(HOMO)}$	-5.328	-5.691	-5.618	-5.473
$E_{(LUMO)}$	-0.361	-0.153	-0.974	-0.954
E_{gap}	4.967	5.538	4.644	4.519
Mulliken charges				
N	-0.672	-0.670	-0.674	-0.638
C8	+0.262	+0.236	+0.218	+0.198
O	-0.475	-0.494	-0.482	-0.472
Q_C-Q_O	+0.737	+0.730	+0.700	+0.670
C7	-0.076	-0.084	-0.079	-0.103

closed forms

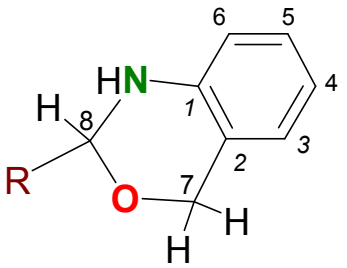

6

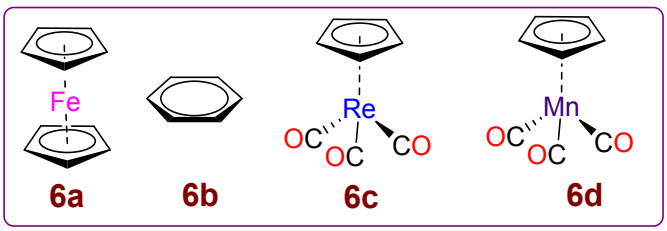

Table S13. Absorption spectroscopic data for compounds in 2-R-2,4-dihydro-1*H*-3,1-benzoxazines (**6a-6d**) in CH_2Cl_2 at 298 K. Wavelengths (λ_i, in nm) and logarithms of the extinction coefficients (log ε_i (ε_i in M^{-1} cm^{-1})].[a]

R	identification code	λ_1	log ε_1	λ_2	log ε_2	λ_3	log ε_3	λ_4	log ε_4
Ferrocenyl	**6a**	302	3.3	284[a]	3.5	245[c]	3.3	228	4.2
Phenyl	**6b**	–	–	284[a]	3.7	240[c]	4.10	228	4.2
Cyrhetrenyl	**6c**	–	–	308	4.3	280	5.26	223	5.6
Cymantrenyl	**6d**	308[b]	4.2	282	4.4	272	4.84	229	5.3

[a] See also Figure S31; [b]according to the bibliography this band is attributed to metal to ligand charge transfer MLCT; [c] Broad; [d] Shoulder.